



U.S. Department
of Transportation
**National Highway
Traffic Safety
Administration**



DOT HS 813 276

September 2022

Crash Simulation of FMVSS No. 214 Safety Performance

DISCLAIMER

This publication is distributed by the U.S. Department of Transportation, National Highway Traffic Safety Administration, in the interest of information exchange. The United States Government assumes no liability for its contents or use thereof. If trade or manufacturers' names or products are mentioned, it is because they are considered essential to the object of the publication and should not be construed as an endorsement. The United States Government does not endorse products or manufacturers.

NOTE: This report is published in the interest of advancing motor vehicle safety research. While the report provides results from research or tests using specifically identified motor vehicle models, it is not intended to make conclusions about the safety performance or safety compliance of those motor vehicles, and no such conclusions should be drawn.

Suggested APA Format Citation:

Reichert, R., Kan, C.-D., & Park, C.-K. (2022, September). *Crash simulation of FMVSS No. 214 safety performance* (Report No. DOT HS 813 276). National Highway Traffic Safety Administration.

Technical Report Documentation Page

1. Report No. DOT HS 813 276	2. Government Accession No.	3. Recipient's Catalog No.	
4. Title and Subtitle Crash Simulation of FMVSS No. 214 Safety Performance	5. Report Date September 2022		6. Performing Organization Code
	8. Performing Organization Report No.		
7. Authors Rudolf Reichert; Cing-Dao Kan; Chung-Kyu Park	10. Work Unit No. (TRAIS)		
9. Performing Organization Name and Address George Mason University Center for Collision Safety and Analysis 4087 University Drive, Suite 2100 Fairfax, VA 22030	11. Contract or Grant No. DTNH2215D00005 693JJ919F000223		
	13. Type of Report and Period Covered Draft Final – Technical Report September 2019 – August 2021		
12. Sponsoring Agency Name and Address National Highway Traffic Safety Administration 1200 New Jersey Avenue SE Washington, DC 20590	14. Sponsoring Agency Code		
	15. Supplementary Notes Prepared for Sanjay Patel (COR) and Reba Dyer (CO), NHTSA		
16. Abstract Federal Motor Vehicle Safety Standard (FMVSS) No. 214 requires doors in applicable vehicles to meet minimum force requirements when subjected to a static load in addition to the occupant protection requirements for the dynamic moving deformable barrier (MDB) and vehicle-to-pole (VTP) tests. The mutual effect of non-compliance was studied using validated finite element models of a 2015 Toyota Camry mid-size sedan and a 2020 Nissan Rogue SUV-type vehicle. It was found that the three configurations engage different main load paths for these vehicles. Consequently, the sedan simulation study indicated that structural modifications that resulted in non-compliance for one of the FMVSS No. 214 load cases did not result in non-compliance for the other two configurations. The SUV simulation study indicated that structural modifications that resulted in non-compliance for one of the load cases did not result in non-compliance for the other two configurations, except for FMVSS No. 214 MDB non-compliance, which also resulted in pole non-compliance. Different metrics from the MDB and pole side impact configurations were evaluated to determine the feasibility of using dynamic performance measurements as a surrogate for the static test. It was found that there are significant limitations to implementing such a strategy, because of the different main load paths relevant for the dynamic and static side impact load cases. Dynamic rigid pole load cell data showed the highest potential of indicating initial door crush resistance.			
17. Key Word FMVSS No. 214, finite element simulation, side impact		18. Distribution Statement Document is available to the public from the DOT, BTS, National Transportation Library, Repository & Open Science Access Portal, rosap.ntl.bts.gov .	
19. Security Classif. (of this report) Unclassified	20. Security Classif. (of this page) Unclassified	21. No. of Pages 58	22. Price

Table of Contents

Executive Summary	1
1. Introduction.....	2
1.1 Background	2
1.2 Research Scope	2
1.3 Objective	2
2. Methods.....	4
2.1 Vehicle Selection	4
2.2 Methodology to Study the Effect of Mutual Non-Compliance	6
2.3 Structural Performance Metric and Injury Mechanism	6
3. Sedan - Toyota Camry Simulation Study	9
3.1 Sedan - MDB Impact Validation	9
3.2 Sedan - Pole Impact Validation	10
3.3 Sedan - Static Door Crush Validation.....	11
3.4 Effect of FMVSS No. 214-S Non-Compliance - Sedan	13
3.5 Effect of FMVSS No. 214 MDB Non-Compliance - Sedan.....	15
3.6 Effect of FMVSS No. 214 Pole Non-Compliance - Sedan.....	17
3.7 Effect of Vehicle Mass.....	18
4. SUV - Nissan Rogue Simulation Study	21
4.1 SUV - Nissan Rogue FE Model Development	22
4.2 SUV - MDB Impact Validation	23
4.3 SUV - Pole Impact Validation	26
4.4 SUV - Static Door Crush Validation	27
4.5 2020 Nissan Rogue Suspension Testing.....	29
4.6 Effect of FMVSS No. 214-S Non-Compliance - SUV	30
4.7 Effect of FMVSS No. 214 MDB Non-Compliance - SUV	31
4.8 Effect of FMVSS No. 214 Pole Non-Compliance - SUV	33
5. Dynamic Performance Measurements as a Surrogate for the Static Test.....	35
5.1 Candidate Dynamic Performance Metrics	35
5.2 Metrics based on Vehicle Accelerometer Data.....	36
5.3 Metrics based on Vehicle and Barrier Deformation	37
5.4 Metrics Based on Rigid Pole Load Cell Data	38
5.5 Surrogate Metrics Limitations	41
6. Conclusion	42
7. References	43
Appendix A. Toyota Camry FE Model Variations.....	A-1
Appendix B. Nissan Rogue FE Model Variations	B-1

Table of Figures

Figure 1. Vehicle categories with different side impact characteristics	4
Figure 2. Process to study effect of mutual non-compliance.....	6
Figure 3. Accelerometer locations	7
Figure 4. MDB velocity and ATD metrics characteristics	8
Figure 5. 2018 vehicle sales by body style	9
Figure 6. Toyota Camry acceleration pulse correlation for (a) vehicle and (b) MDB.....	10
Figure 7. Toyota Camry exterior crush correlation	10
Figure 8. Toyota Camry pole impact – Setup pre-crash.....	11
Figure 9. Toyota Camry pole impact – Post-crash	11
Figure 10. Toyota Camry pole impact test versus simulation correlation	11
Figure 11. (a) FMVSS 214-S setup; (b) Typical load displacement plot; (c) Criteria.....	12
Figure 12. FMVSS 214-S validation (a) with seat; (b) without seat	12
Figure 13. FMVSS No. 214-S (a) setup; (b) structural modifications; (c) force comparison	13
Figure 14. Effect of FMVSS No. 214-S non-compliance for 214-MDB.....	14
Figure 15. Effect of FMVSS No. 214-S non-compliance for 214-Pole.....	14
Figure 16. FMVSS No. 214-MDB (a) modifications and (b) crosssection view	15
Figure 17. Effect of FMVSS No. 214-MDB non-compliance for 214-S.....	16
Figure 18. Effect of FMVSS No. 214-MDB non-compliance for 214-Pole.....	16
Figure 19. Effect of FMVSS No. 214-S non-compliance for 214-Pole.....	17
Figure 20. Effect of FMVSS No. 214-Pole non-compliance for 214-S.....	17
Figure 21. Effect of FMVSS No. 214-Pole non-compliance for 214-MDB.....	18
Figure 22. Effect of GVWR for FMVSS No. 214-MDB.....	19
Figure 23. Effect of GVWR for FMVSS No. 214-Pole.....	20
Figure 24. MDB impact location relative to sill and occupant (a) SUV; (b) sedan.....	21
Figure 25. U.S. vehicle segment (a) market share; (b) change in annual sales (2013-2018)	22
Figure 26. Reverse engineering FE vehicle model development process	23
Figure 27. Vehicle tear-down and FE model development process	23
Figure 28. 2020 Nissan Rogue FMVSS No. 214 MDB test.....	24
Figure 29. FMVSS No. 214 MDB validation (a) top view; (b) velocity crash pulse	24
Figure 30. (a) 53 km/h FMVSS No. 214 MDB occupant test versus simulation.	25
Figure 30. (b) 62 km/h MDB occupant test versus simulation.....	26

Figure 31. Nissan Rogue FMVSS No. 214 pole post-crash (a) top; (b) side view	27
Figure 32. FMVSS No. 214 pole validation (a) velocity crash pulses; (b) top view	27
Figure 33. Nissan Rogue FMVSS No. 214 static post crash (a) front door; (b) rear door	28
Figure 34. FMVSS No. 214 static door crush validation (a) front; (b) rear door	28
Figure 35. Nissan Rogue Suspension Testing.....	29
Figure 36. (a) FMVSS No. 214-S non-compliance; (b) effect for 214-MDB load case.....	30
Figure 37. FMVSS No. 214-S non-compliance; (b) effect for pole impact load case.....	31
Figure 38. FMVSS No. 214-MDB non-compliance; (b) effect for FMVSS No. 214-S load case.....	32
Figure 39. (a) FMVSS No. 214 MDB non-compliance; (b) effect for pole impact load case.....	32
Figure 40. (a) FMVSS No. 214-S non-compliance; (b) effect for 214 Pole load case	33
Figure 41. SUV (a) FMVSS No. 214 Pole non-compliance; (b) effect for MDB load case	34
Figure 42. Candidate structural metrics from dynamic tests as surrogate for static test	35
Figure 43. SUV Accelerometer Data - Baseline versus 214-static Non-compliant (a) B-Pillar Velocity; (b) Relevant Locations; (c) Door Velocity	37
Figure 44. Deformation-based metrics (a) MDB deformation; (b) IIHS structural criteria; (c) exterior vehicle crush.....	38
Figure 45. Deformation-based metrics (a) MDB deformation; (b) IIHS structural criteria and exterior vehicle crush.....	38
Figure 46. Sequence of FMVSS No. 214 pole characteristic crash events using a crosssection view.....	39
Figure 47. Pole impact force time history data for rocker, door, and roof area.....	39
Figure 48. Nissan Rogue baseline versus FMVSS No. 214-S static non-compliant model (a) comparison of static door crush resistance force; (b) load cell locations; (c) comparison of force versus deformation at the door location.....	40
Figure 49. Main load paths during FMVSS No 214 (a) pole; (b) MDB; and (c) static door crush.....	42
Figure A-1. Toyota Camry FMVSS No. 214 static non-compliant versus baseline model.....	A-2
Figure A-2. Toyota Camry FMVSS No. 214 MDB non-compliant versus baseline model.....	A-2
Figure A-3. Toyota Camry FMVSS No. 214 pole non-compliant versus baseline model	A-3
Figure B-1. Nissan Rogue FMVSS No. 214 static non-compliant versus baseline model.....	B-2
Figure B-2. Nissan Rogue FMVSS No. 214 MDB non-compliant versus baseline model	B-3
Figure B-3. Nissan Rogue FMVSS No. 214 pole non-compliant versus baseline model	B-4

Table of Tables

Table 1. Crossover vehicles with highest U.S. sales number in 2018	22
Table 2. Rogue FMVSS No. 214 static door crush resistance forces (a) front; (b) rear door	29

Executive Summary

Federal Motor Vehicle Safety Standard (FMVSS) No. 214 requires doors in applicable vehicles to meet minimum force requirements when subjected to a static load in addition to the occupant protection requirements for the dynamic moving deformable barrier (MDB) and vehicle-to-pole (VTP) tests. This study explores the option of developing performance criteria so that results from the FMVSS No. 214 dynamic MDB and/or VTP tests could be used for the static door crush resistance requirements of FMVSS No. 214.

Finite element (FE) models of a Toyota Camry sedan and Nissan Rogue SUV were used to conduct this research. The 2015 sedan FE model existed from previous research and the 2020 SUV FE model was developed using a reverse engineering process. Existing full-scale tests for the MDB and VTP impacts have been used to validate the FE models. The models were further validated using FMVSS No. 214 static door crush tests, which were conducted in cooperation with the Transportation Research Center (TRC) and dynamic MDB and pole tests conducted in cooperation with Calspan Corporation. The FE models showed good correlation between test and simulation for all three FMVSS No. 214 impact configurations. The validated FE models, which represent the sedan and SUV vehicle classes, were then used to conduct simulation studies with design modifications that met or only partially met FMVSS No. 214 static and dynamic test requirements.

The Toyota Camry sedan simulation study demonstrated that the three FMVSS No. 214 configurations engage different main load paths: (1) the static door crush performance mainly relied on the door beam and connections at the door hinges and lock; (2) the dynamic MDB configuration mainly relied on the B-pillar strength; and (3) sill and floor components were most important for the pole side impact. Simulation results indicated that structural modifications that resulted in non-compliance for one of the load cases did not result in non-compliance for the other two configurations. The results for the sedan vehicle class were presented at the 2021 SAE Government Industry Meeting (Reichert, 2021).

A similar simulation study was conducted using a Nissan Rogue FE model. The SUV class presents different crash characteristics compared to sedans due to more overlap of the sill and the MDB as well as higher occupant seating position. The SUV study indicated that structural modifications that resulted in non-compliance for one of the load cases did not result in non-compliance for the other two configurations, except for MDB non-compliance, which also resulted in pole non-compliance.

Different metrics from the MDB and pole side impact configurations were evaluated to determine the feasibility of using dynamic performance measurements as a surrogate for the static test. Metrics included (1) structural velocities based on accelerometer data from the B-pillar and door; (2) deformation-based data from the vehicle exterior crush, B-pillar intrusion, and MDB honeycomb deformation; and (3) rigid pole load cell time history data. It was found that there are significant limitations to using dynamic measurements as surrogate for the static door crush test, because different main load paths are engaged during the dynamic and static side impact requirements. Dynamic rigid pole load cell data showed the highest potential of indicating initial door crush resistance.

1. Introduction

1.1 Background

FMVSS No. 214 requires doors in applicable vehicles to meet minimum force requirements when the door is statically loaded (crushed) by a rigid steel cylinder or semi-cylinder. Additionally, FMVSS No. 214 requires occupant protection during dynamic moving deformable barrier and vehicle-to-pole tests. This project explores options for developing performance criteria so that the FMVSS No. 214 dynamic MDB and/or VTP tests could be used as replacements for the static door crush resistance requirements of FMVSS No. 214, thus allowing the static requirements to be eliminated without reducing safety. Neither of the existing dynamic FMVSS No. 214 test procedures measure door crush resistance force.

1.2 Research Scope

The scope of this project consisted of developing, validating, and using detailed finite element models for use in side impact test procedures for two vehicles with different side impact characteristics. The FE models were to be used to compare intrusions, applied forces, and occupant injury metrics among baseline and modified vehicle simulations. The vehicle modifications were to be developed to meet or only partially meet FMVSS No. 214 static and dynamic test requirements. The results were then to be evaluated to consider the feasibility of using the dynamic performance measurements as a surrogate for the static test.

1.3 Objective

The objective of this research was to use and develop detailed FE vehicle models to simulate FMVSS No. 214 static door crush, dynamic MDB, and VTP test conditions. The baseline FE simulations were to be validated against test data where available. Testing was to be conducted or contracted to provide additional validation data where needed. In addition to the baseline validation, three model variations were to be developed to demonstrate non-compliance with a single test condition. Simulations for each model variation were to be performed in each of the three test conditions. The simulation results for the modified vehicle models had to be analyzed to consider how non-compliance with a single test condition affects the compliance and test performance of the other two test conditions. Additionally, the feasibility of dynamic measurements that could be considered as a surrogate for the static test procedure had to be evaluated, if applicable.

Specifically, the objectives were the following.

- Devise at least two different vehicles for side crash simulation development and testing. The vehicle selection should consider the diversity of vehicle geometry, design, and crash kinematics.
- Where required purchase vehicles, measure and conduct testing to support the development and validation of simulation models.
- FE models shall be developed for the selected vehicles in each of the three test conditions. Each model shall be validated against test data. Objective rating methods shall be used to evaluate the correlation between test and simulation results. For the

dynamic tests, it is sufficient to validate against the vehicle intrusion and intrusion velocity measurements rather than the resulting occupant injury criteria.

- Develop, simulate, and evaluate vehicle modifications. The first modifications will demonstrate minimal non-compliance to the static FMVSS No. 214 test. Simulations will be performed to evaluate how non-compliance affects the vehicle response in the MDB and VTP tests.
- Similarly, develop modifications that produce minimal non-compliance with the MDB and VTP dynamic FMVSS No. 214 configurations. Evaluate how this would affect the vehicle response in the static and VTP/MDB test, respectively.
- Evaluate the simulation results for compliant and non-compliant vehicle models and evaluate the feasibility of using measurements from the dynamic tests to predict compliance with the static 214 test requirements.

2. Methods

2.1 Vehicle Selection

FMVSS No 214 static door crush and dynamic Pole requirements apply to vehicles with a Gross Vehicle Weight Rating (GVWR) up to 10,000 pounds, while the FMVSS No. 214 MDB compliance is required for passenger cars with GVWRs up to 10,000 pounds but to multipurpose passenger vehicles, trucks and buses with a GVWR up to 6,000 pounds. Vehicles with a GVWR above 6,000 pounds were not considered for this research. The identification of two different vehicles was important to assess variations in vehicle designs. The criteria that were used to identify the most suitable vehicle types for this research are outlined below.

Geometry and Side Crash Characteristics

The first vehicle selection criteria included the evaluation of design concepts and side crash characteristics. Different vehicle geometries and classes show significantly different behavior in side impact in general and in FMVSS No. 214 configurations in particular. Three vehicle types/classes, which represent the most important differences in crash kinematics due to vehicle and sill height, vehicle mass, and door length were considered, as shown in Figure 1.



Figure 1. Vehicle categories with different side impact characteristics

1. Four-door sedan

This vehicle class was important for this research, representing a large percentage of vehicles on the road. Typically, the MDB partially overrides and does not engage the sill of the vehicle and loads are transferred into the door and B-pillar.

2. Pickup or SUV

This vehicle class can be less critical with respect to occupant protection in the MDB configuration. Due to the different vehicle dimensions and higher occupant seating position, the MDB typically engages with the sill area of the vehicle. Loads are transferred into the sill/floor, the door, and the B-pillar. In contrast, VTP configurations can be more critical compared to sedans, due to the higher vehicle mass, which can result in higher forces and intrusions. Two different pole locations can be tested according to FMVSS No. 214: the first one is aligned with the head of the 5th percentile occupant in a more forward seating position, the second one is positioned to hit the head of a 50th percentile occupant in a longitudinal mid position. The more forward position was considered more critical with respect to vehicle intrusion criteria.

3. Two-door sedan coupe or convertibles

While the overall sales numbers are smaller than for the previously described vehicle types, the two-door coupe type vehicles often have longer doors and can present challenges in side impact protection. Specific structural countermeasures and restraint system solutions are needed to overcome these challenges.

Sales Numbers and Rating Results

The second vehicle selection criteria included sales numbers and rating results. An analysis was performed on how well a candidate vehicle represents cars in the US market and how well the vehicle performed in side impact consumer information crash tests. A vehicle with higher sales numbers was considered a better candidate vehicle for this study. All applicable vehicles on U.S. roads fulfill the FMVSS No. 214 requirements. Differences exist in side impact NCAP (SINCAP) and Insurance Institute for Highway Safety (IIHS) rating tests. Vehicles with higher ratings were considered to have better structural design and are therefore more likely to be used in future vehicle structures and hence were judged better candidates for inclusion in this research.

Availability of Test Results

The third vehicle selection criteria included the availability of test results for the respective impact configurations. Vehicle manufacturers (original equipment manufacturers, OEMs) conduct all three FMVSS No. 214 tests for compliance reasons. Publicly available test results are limited for the FMVSS No. 214 quasistatic door crush and the 54 km/h dynamic MDB configuration. Pole tests exist for most vehicles with high sales numbers, such as the Toyota Camry, Honda Accord, and Nissan Rogue. OEMs typically use the 62 km/h MDB SINCAP rating test to ensure compliance with the FMVSS No. 214 MDB test at 54 km/h during the vehicle development phase. SINCAP MDB tests at 62 km/h are publicly available for most vehicles with high sales numbers. The results from the identical impact configuration at higher speed were used for model validation. Vehicle-to-pole tests for the 5th percentile seating position were considered more suitable for the intended study since the impact location is closer to the middle of the door. Missing test results were generated in cooperation with TRC in Ohio and Calspan in Michigan.

Availability of FE models

Several publicly accessible FE vehicle models are available from NHTSA (www.nhtsa.gov/crash-simulation-vehicle-models). The models were developed using a reverse engineering process. FE model examples include the 2015 Toyota Camry, the 2014 Honda Accord, and the 2018 Dodge Ram. A candidate vehicle model for this study was the detailed Toyota Camry FE model. A vehicle would be a good candidate for this study if a baseline model is already available and has been used and validated in previous studies. An available FE model of the 2018 Ram was considered, but dismissed because of a GVWR above 6,000 lbs. Instead, a FE model of the popular crossover SUV vehicle class, a 2020 Nissan Rogue was developed, using a reverse engineering process in course of this research.

2.2 Methodology to Study the Effect of Mutual Non-Compliance

The baseline simulation model was validated using test data from the three FMVSS No. 214 impact configurations, and then modified to produce non-compliance for one of the requirements. Using the modified simulation model, the effect on the other two impact configurations was studied, as shown in Figure 2.

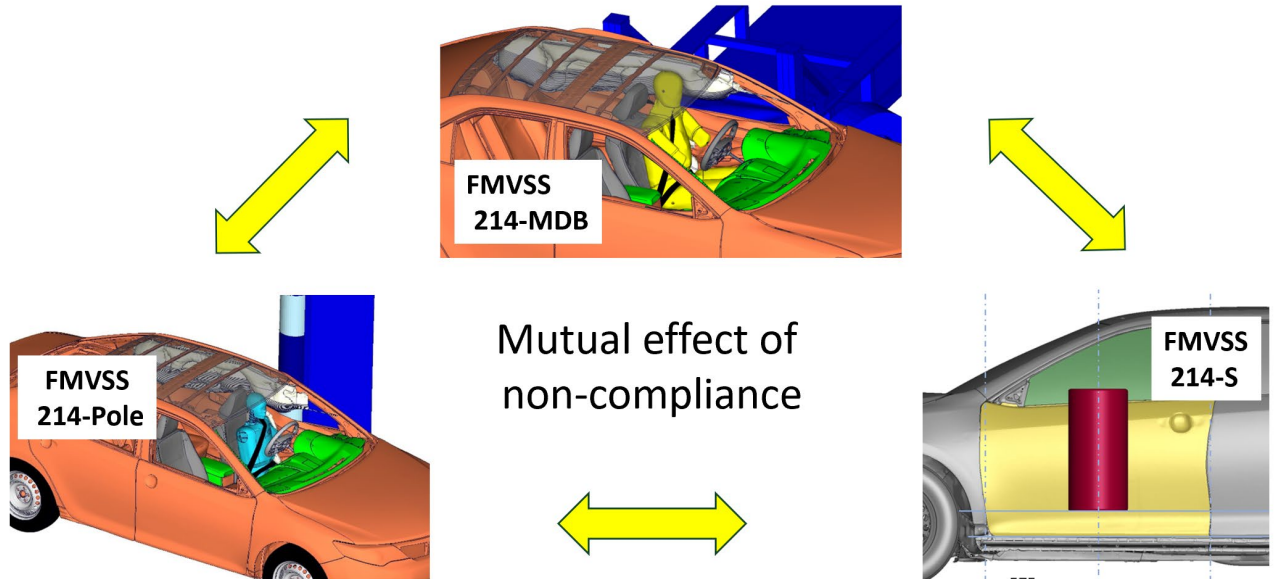


Figure 2. Process to study effect of mutual non-compliance

The first modifications demonstrated minimal non-compliance to the static FMVSS No. 214 condition. Simulations were then performed to evaluate, how this non-compliance affected the vehicle response in the MDB and VTP conditions. Similarly, FE model variations that showed non-compliance for the MDB and VTP dynamic FMVSS No. 214 configurations were developed, and an evaluation was performed on how this would affect the vehicle response in the static and other dynamic impact configuration.

Observations that were made during the validation process and experience from previous side impact projects were used to determine reasonable structural modifications that produced the intended non-compliance for the respective impact condition. The simulation studies included the analysis of vehicle intrusion, vehicle pulse, and force criteria for the baseline and the modified simulation models.

Since dynamic FMVSS No. 214 MDB and pole impact compliance is based on anthropomorphic test device (ATD) metrics, select simulations were conducted using validated models of 5th and 50th percentile side impact dummies, to verify the trends observed from the structural analyses.

2.3 Structural Performance Metric and Injury Mechanism

Velocity pulses at relevant vehicle locations, recorded by accelerometers, are a good indicator of structural performance in the FMVSS No. 214 MDB configuration, where the moving barrier impacts the stationary vehicle. From the author's experience working in industry and with major car manufacturers it is known that the B-pillar thorax location is used by some OEMs to judge the structural side impact performance of a vehicle. An accelerometer positioned at the middle of

the B-pillar provides important information with respect to occupant loads caused by vehicle deformation and vehicle kinematics. In frontal impact configurations, interaction of the occupant with the seat and seat belt results in deceleration of the occupant coupled with the vehicle deceleration, called ride-down effect. Side impact injury mechanisms are different. In a collision where an occupied stationary vehicle is impacted by a striking vehicle from the side, occupant loads are mainly induced by the deformation of the vehicle structure and interior and the motion of the near side structure. The absolute B-pillar velocity describes the combination of the vehicle deformation and vehicle motion and is therefore a good indicator for loads relevant for occupant injury risk, which are then mainly mitigated by optimized air bags and interior components. To further explain the side impact characteristic, we can assume two extreme cases, (1) a small vehicle with low mass and no significant deformation, and (2) a heavy vehicle with a significant amount of deformation. The light vehicle would be pushed away during an impact and the heavy vehicle would not move but experience near-side structural deformation, while the occupant predominantly remains at the initial location without significant ride-down effect. The absolute velocity measured at the B-pillar is a good structural metric in side impact, because it captures well the load the occupant experiences for both cases, in the first case caused by vehicle motion, and in the second case mainly caused by vehicle deformation. Similarly, absolute velocities measured at the doors can be a good indicator for a vehicle's side impact performance, while measurements from the doors are more likely to show questionable data in full-scale testing, due to local buckle effects and higher oscillations, compared to the B-pillar location. Figure 3 shows locations that were analyzed during this research.

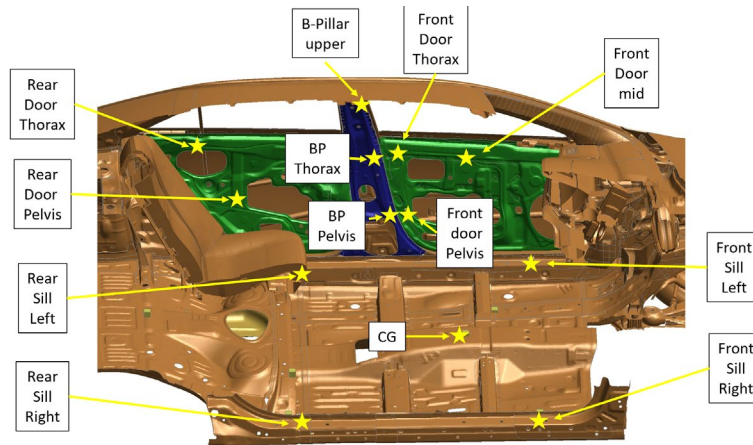


Figure 3. Accelerometer locations

The B-pillar and door locations are of special interest due to their proximity with the occupant's contact areas. Figure 4 shows an example of a door velocity and a driver's pelvis force profile. Later contact, i.e., larger initial dummy to interior clearance and lower velocity typically correlates with lower injury risk. Local effects, due to interior design and restraints also play an important role.

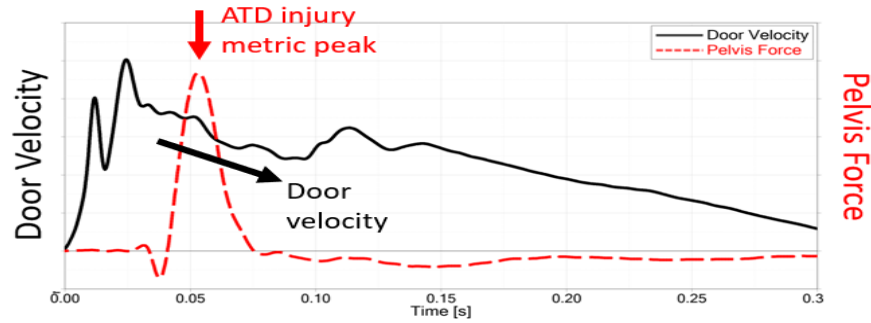


Figure 4. MDB velocity and ATD metrics characteristics

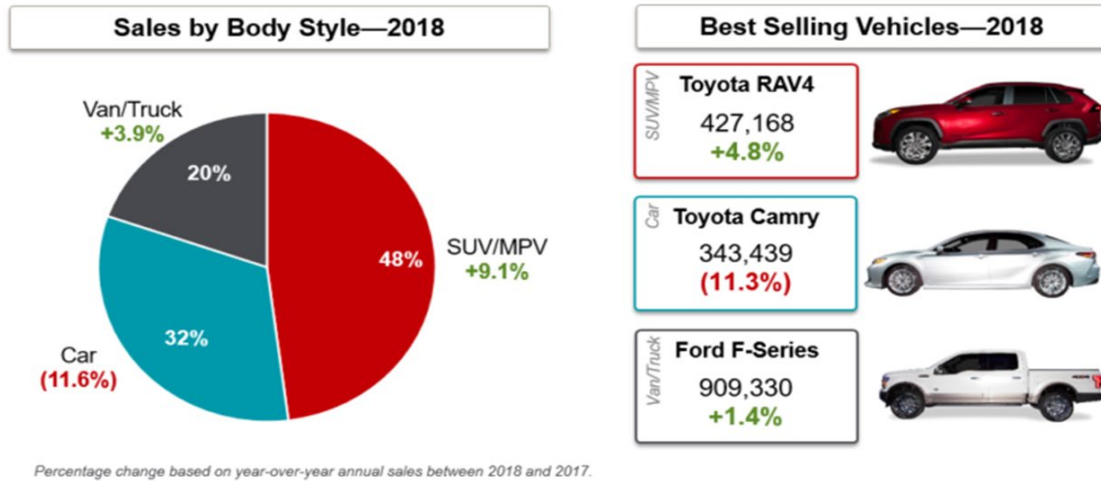
In contrast, during the FMVSS No. 214 pole configuration, the vehicle is positioned on a so-called “flying floor” and moves into the stationary rigid pole, which is aligned with the driver’s head center of gravity. The vehicle is promptly decelerated and the velocity profiles at the door and B-pillar highly depend on the distance from the impact location. Therefore, the velocity profiles are less relevant in this configuration. Local effects involving the ATD, interior, and restraints play an important role.

Deformation and force versus deformation characteristics were monitored. Remaining occupant compartment space is another criterion, which is often used to judge the structural performance during a side impact, whereas deformation and contact characteristics in the early phase of the impact are relevant for FMVSS No. 214 ATD criteria. The force versus deformation criteria was used to judge the performance in the FMVSS No. 214 static (S) configuration.

3. Sedan - Toyota Camry Simulation Study

The 2015 Toyota Camry was selected for this research, representing the 4-door sedan vehicle class with a low sill as well as a door and B-pillar design characterizing many sedan vehicles. It has been one of the top selling vehicles in the United States in recent years, including 2018, as shown in Figure 5.

U.S. 2018 sales and best-selling vehicles by body style JATO



© JATO Dynamics Ltd

Figure 5. 2018 vehicle sales by body style

The Toyota Camry received a 5-Star SINCAP and a “GOOD” IIHS crash rating for the 2015 as well as for the 2020 model year. FMVSS No. 214 pole and SINCAP MDB test data exists, and a detailed FE model of a Toyota Camry was previously developed using a reverse engineering process (Reichert et al., 2016; Reichert & Kan, 2017).

3.1 Sedan - MDB Impact Validation

Results from an existing MDB SINCAP test (NHTSA # 9001, 2015 Toyota Camry) were used to validate the existing Toyota Camry FE model. The MDB was positioned according to the FMVSS No. 214 test procedure. Simulations were conducted with an impact velocity of 62 km/h. Crash pulses from test and simulation were compared using the objective rating tool CORA (Thunert, 2012). CORA rating scores range between 0 and 1, where 0 means no correlation and 1 means (close to) perfect correlation. Specifically, a CORA rating (Barbat et al., 2015) greater than 0.94 was considered excellent, values between 0.8 and 0.94 represented good, and values between 0.58 and 0.8 represented fair correlation.

CORA values of 0.86 and 0.94 for vehicle and barrier acceleration pulses documented good to excellent correlation between test and simulation, respectively, as documented in (Reichert & Kan, 2017) and shown in Figure 6.

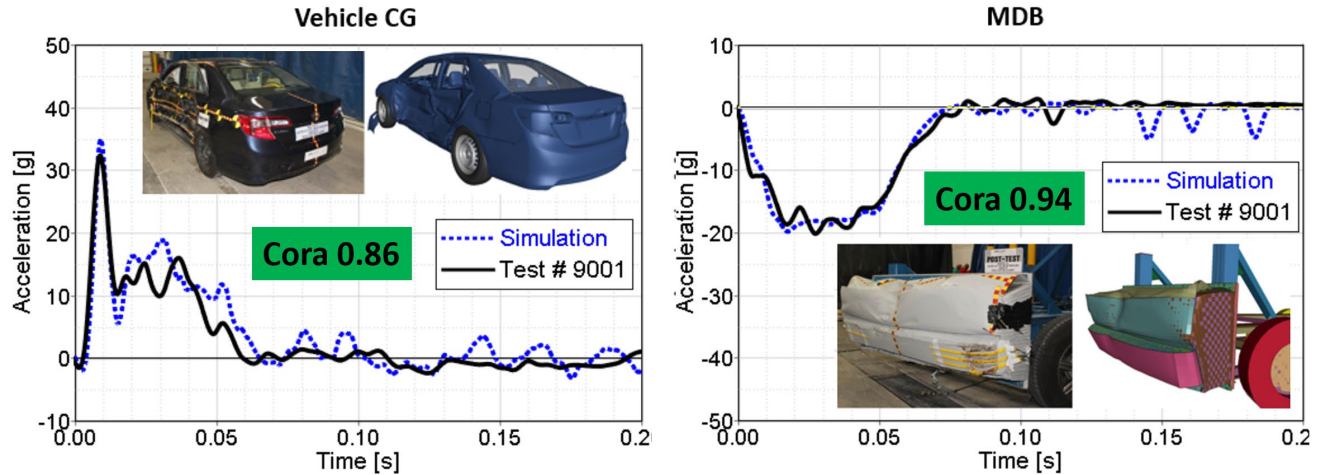


Figure 6. Toyota Camry acceleration pulse correlation for (a) vehicle and (b) MDB

Deformation of the MDB honeycomb face showed similar characteristics for test and simulation, such as (1) downward tilting of the bumper and (2) higher deformation at the area that impacted the B-pillar, as shown in Figure 6 (b).

Exterior crush was measured at five different heights of the vehicle, i.e. the sill, the height of the occupant hip point (H-point), the mid door location, close to window opening, and at the roof. The largest exterior crush was observed at locations 2 and 3 at the doors. The maximum value of 264 mm in the simulation compared reasonably well with the maximum value of 249 mm from the full-scale test, as shown in Figure 7.

Suspensions were modelled using experience from previously conducted tests at the Federal Outdoor Impact Laboratory (FOIL).

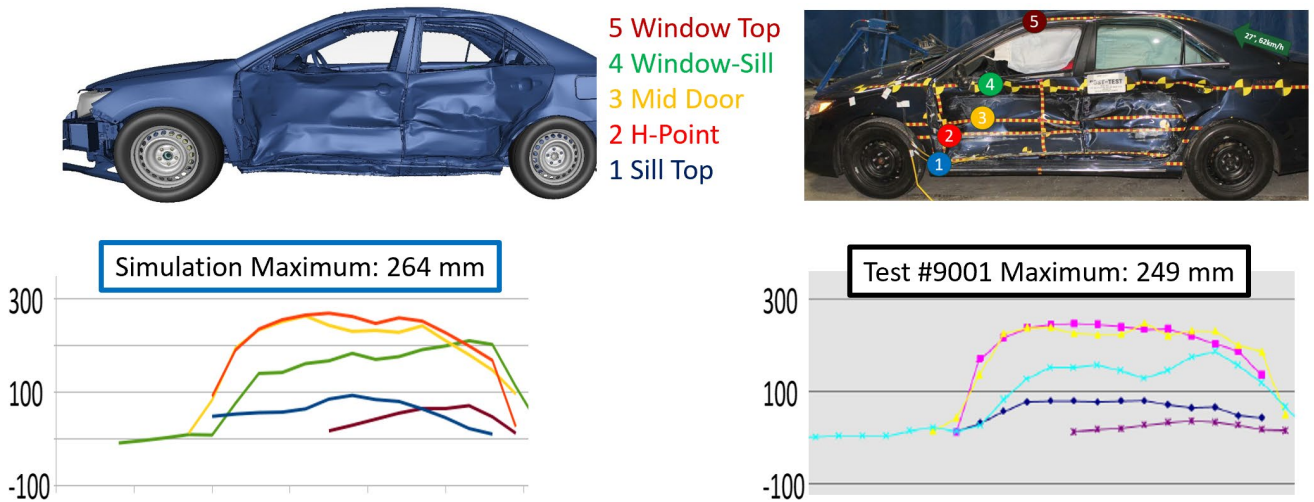


Figure 7. Toyota Camry exterior crush correlation

3.2 Sedan - Pole Impact Validation

Results from an existing FMVSS No. 214 pole test (NHTSA # 8558, 2014 Toyota Camry), were used to validate the existing Toyota Camry FE model. Figure 8 shows the side view pre-crash in

test and simulation. The vehicle was positioned at a 75° angle and impacted the stationary rigid pole according to the FMVSS No. 214 pole impact specification with 32 km/h.



Figure 8. Toyota Camry pole impact – Setup pre-crash

Figure 9 shows a top view of the exterior crush profile. The maximum value of 380 mm in the simulation compared well with the maximum value of 379 mm from the full-scale test.

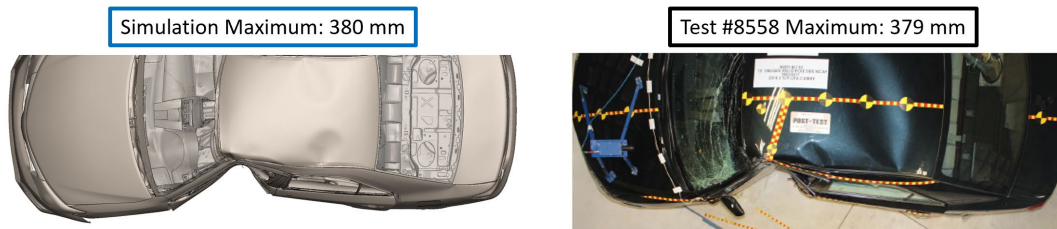


Figure 9. Toyota Camry pole impact – Post-crash

Crash pulses from test and simulation were compared using the objective rating tool CORA. A value of 0.96 for the comparison of the velocity pulse at the vehicle center of gravity documents excellent correlation, as shown in Figure 10.

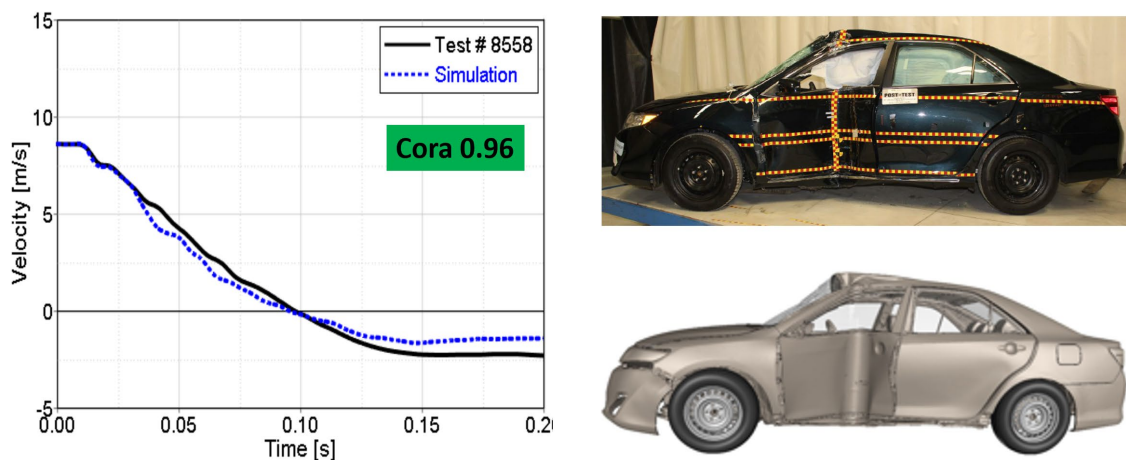


Figure 10. Toyota Camry pole impact test versus simulation correlation

3.3 Sedan - Static Door Crush Validation

FMVSS No. 214-S requires doors in applicable vehicles to meet minimum force requirements when the front and rear door is quasi-statically loaded with a rigid steel cylinder, as shown in Figure 11 (a). A typical force versus displacement plot is shown in Figure 11 (b). The initial and

intermediate crush resistance values represent the average force to deform the door (area under force versus displacement curve divided by 6 / 12 inches). Minimum resistance force criteria depend on the test setup, i.e. with or without seats installed. A higher door crush resistance force is required for setups with seats installed, as shown in Figure 11 (c).

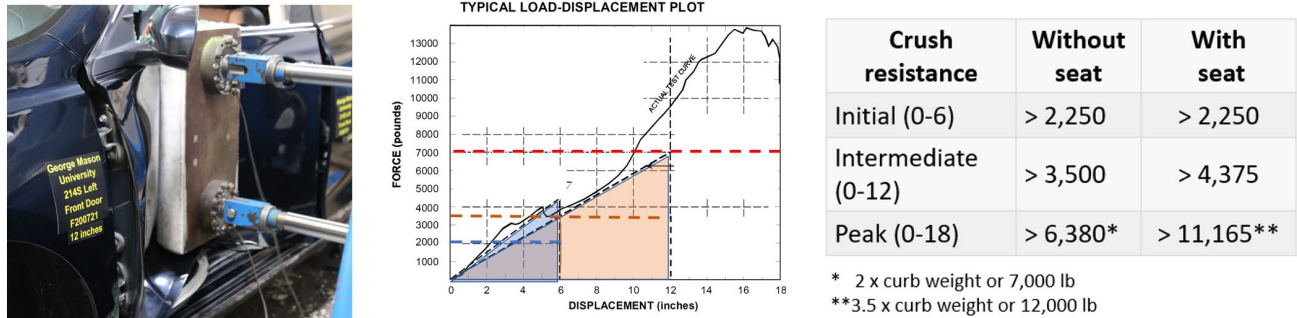


Figure 11. (a) FMVSS 214-S setup; (b) Typical load displacement plot; (c) Criteria

FMVSS No. 214-S door crush tests were conducted at the TRC in Ohio. A 2017 Toyota Camry representing the 2015 model year was purchased. The left front driver door was used to conduct the quasi-static door crush test with seat installed and the right front door was used to generate test data without seat. Figure 12 (a) and (b) show the comparison of test and baseline simulation with and without seat, respectively. The entire range of displacement until 18 inches was evaluated. Good correlation of the force versus displacement time history data was achieved represented by CORA scores of 0.90 and 0.93. Initial, intermediate, and peak resistance forces were well captured and showed values above the relevant required minimum criteria in test and simulation.

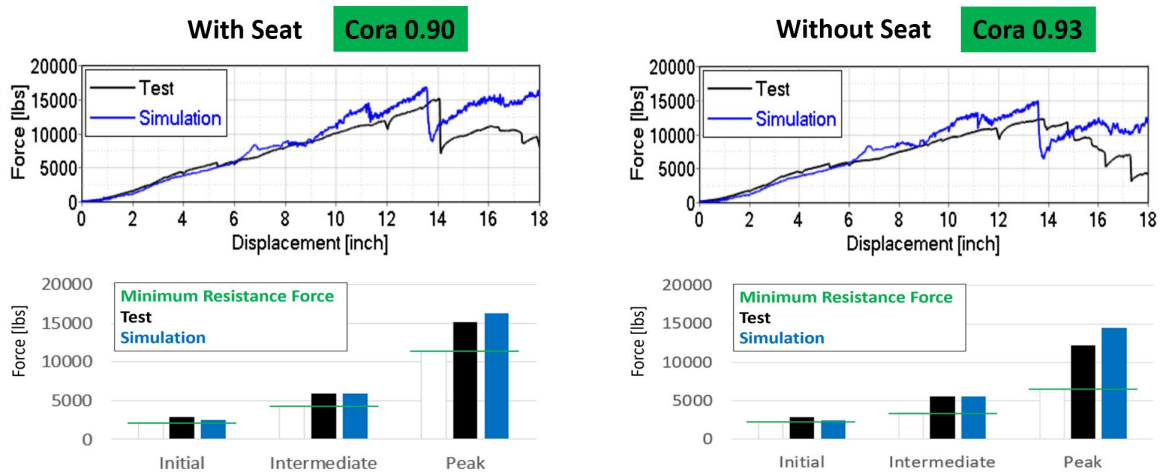


Figure 12. FMVSS 214-S validation (a) with seat; (b) without seat

The baseline FE model was also validated using test data for the rear door. The test was automatically stopped after about 8 inches because the load cell had reached 95 percent of its capacity. Simulation and test results correlated well, represented by a CORA score of 0.91. All simulations were conducted using explicit time integration method used for dynamic crash applications. LS-Dyna also allows to run simulations using implicit time integration, appropriate

for events that are much slower, and the effects of strain rates are minimal. To run the FE models using the implicit method, model modifications are needed. For consistency reasons, the explicit method with a relatively large, i.e., 2 second, termination time, was also used for the static door crush test. Similar approaches are being used when evaluating roof strength. Differences for using implicit versus explicit time integration are considered small for these cases.

The Toyota Camry baseline FE model, which represents the 2012 and 2015 physical vehicles with respect to side impact performance, can be downloaded from GMU/CCSA’s vehicle model website, www.ccsa.gmu.edu/models/.

3.4 Effect of FMVSS No. 214-S Non-Compliance - Sedan

The validated sedan baseline model was first modified in such a way that it showed non-compliance based on the minimum door crush resistance force criteria. It was found from the validation results that the initial FMVSS No. 214-S force requirement, defined for the first six inches of deformation, had the smallest margin to the minimum resistance force criteria, compared to the intermediate and peak resistance force criteria. According to the defined test procedure, the cylindrical impactor does not overlap with the sill of the vehicle, as shown in Figure 13 (a). The door beam and the integrity of the door to B-pillar lock connections were found to have a significant effect on the FMVSS No. 214-S performance. Consequently, non-compliance was achieved by reducing the strength of the door beam, as shown in Figure 13 (b), and documented in Appendix A1. The resulting initial resistance force for the first 6 inches of deformation using the modified FE model was below the required minimum force criteria, as shown by the red bar in Figure 13 (c). The intermediate resistance force showed a borderline value and was lower than in the baseline simulation. The peak resistance force was lower than in the baseline simulation as well but above the required minimum peak force requirement. Similar observations were made for the analysis with removed seat.

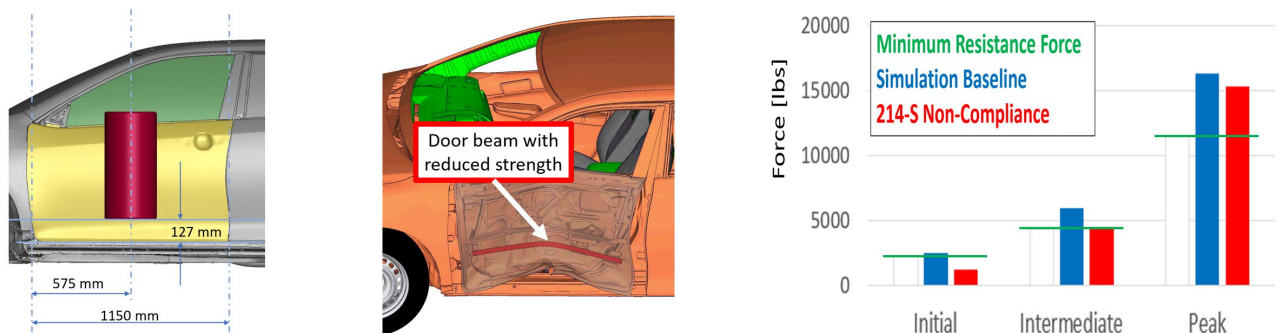


Figure 13. FMVSS No. 214-S (a) setup; (b) structural modifications; (c) force comparison

The model that showed non-compliance for the FMVSS No. 214-S test configuration was then exercised in the FMVSS No. 214 MDB condition, as shown in Figure 14. Structural modifications that resulted in FMVSS No. 214-S non-compliance resulted in marginally higher maximum velocity at the B-pillar and front door. Similarly, simulations with a 50th percentile WorldSID dummy, developed by the Partnership for Dummy Development and Biomechanics, in the driver seat indicated that the maximum chest deflection was marginally higher, while clearly below the defined reference criteria. The conducted simulations indicated FMVSS No. 214 MDB compliance despite 214-S non-compliance.

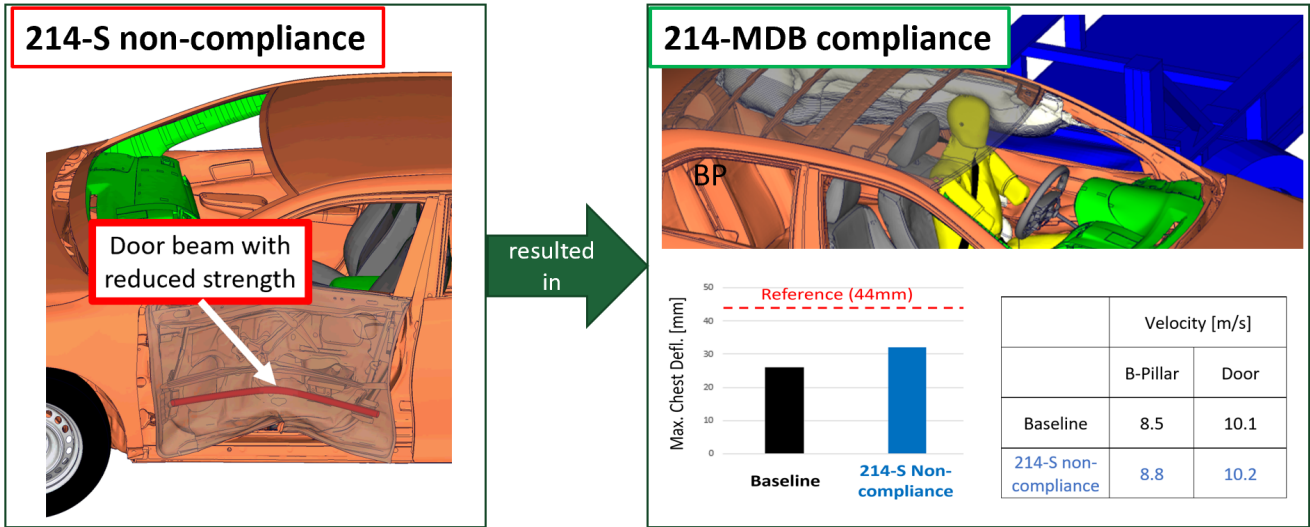


Figure 14. Effect of FMVSS No. 214-S non-compliance for 214-MDB

The model that showed non-compliance for the FMVSS No. 214-S test configuration was then exercised in the FMVSS No. 214 pole condition, as shown in Figure 15. Structural modifications that resulted in FMVSS No. 214-S non-compliance resulted in similar structural deformation in the 214-pole configuration as the FMVSS No. 214-S compliant baseline version. The maximum exterior crush was marginally higher. Similarly, simulations with a 5th percentile SID-IIIs dummy model, developed by ANSYS LSTC, in the driver seat indicated that the maximum combined pelvis force was similar to the baseline simulation, clearly below the defined reference criteria. The conducted simulations indicated FMVSS No. 214-pole compliance despite 214-S non-compliance.

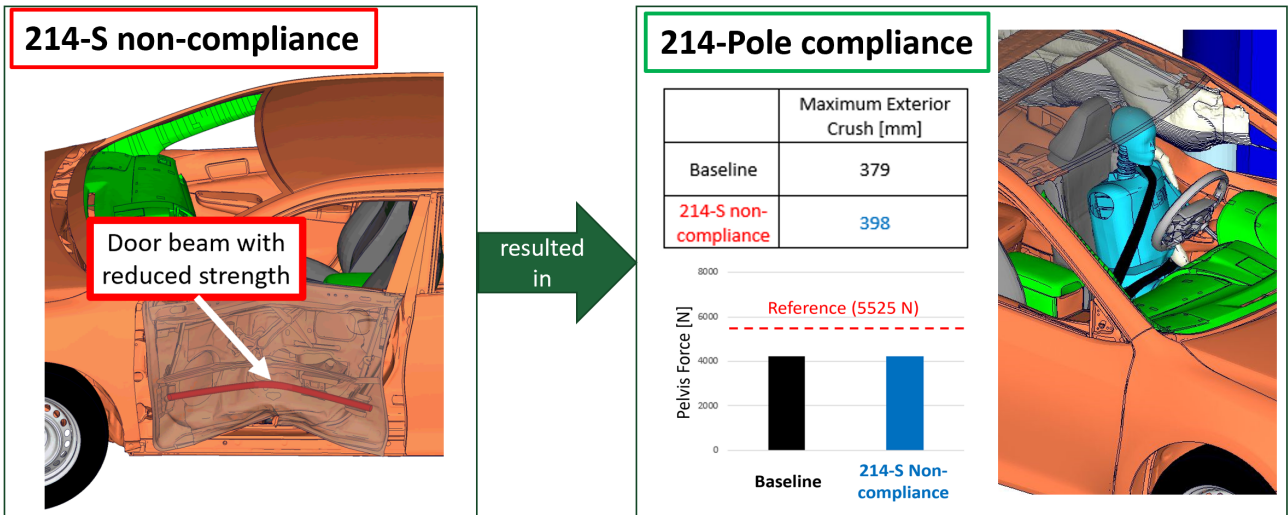


Figure 15. Effect of FMVSS No. 214-S non-compliance for 214-Pole

The reduced strength for door beam, that resulted in 214-S non-compliance did not significantly affect the performance in the 214-MDB condition which mainly relies on B-pillar components.

Similarly, it did not significantly affect the performance in the 214-Pole condition, where the vehicle impacts the pole at the front door overlapping with the sill.

In conclusion, the conducted simulations with a validated sedan FE model indicated FMVSS No. 214 MDB and 214 pole compliance despite FMVSS No. 214-S non-compliance.

3.5 Effect of FMVSS No. 214 MDB Non-Compliance - Sedan

The validated Toyota Camry FE baseline model was modified in such a way that it showed non-compliance for the FMVSS No. 214 MDB configuration. Figure 16 (a) shows the parts with reduced strength in red. The structural B-pillar components play an important role for the MDB condition. This is especially true for the sedan vehicle with no significant overlap of the vehicle sill and the barrier bumper, as shown in the cross-section view in Figure 16 (b).

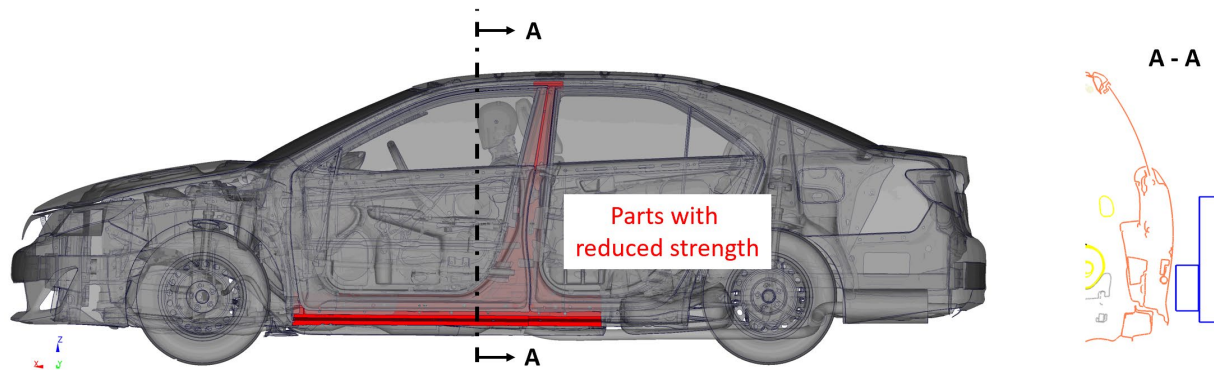


Figure 16. FMVSS No. 214-MDB (a) modifications and (b) crosssection view

A detailed comparison of modified parts is documented in Appendix A2. The model that showed non-compliance for the FMVSS No. 214 MDB configuration was then exercised in the FMVSS No. 214-S static door crush condition, as shown in Figure 17. Structural modifications that resulted in FMVSS No. 214 MDB non-compliance resulted in marginally lower initial and intermediate force levels in the quasi-static configuration. Values were marginally lower than for the baseline FE model, but above the minimum required resistance force, defined for FMVSS No. 214 compliance. The conducted simulations indicated FMVSS No. 214-S door crush resistance force compliance despite dynamic 214-MDB non-compliance.

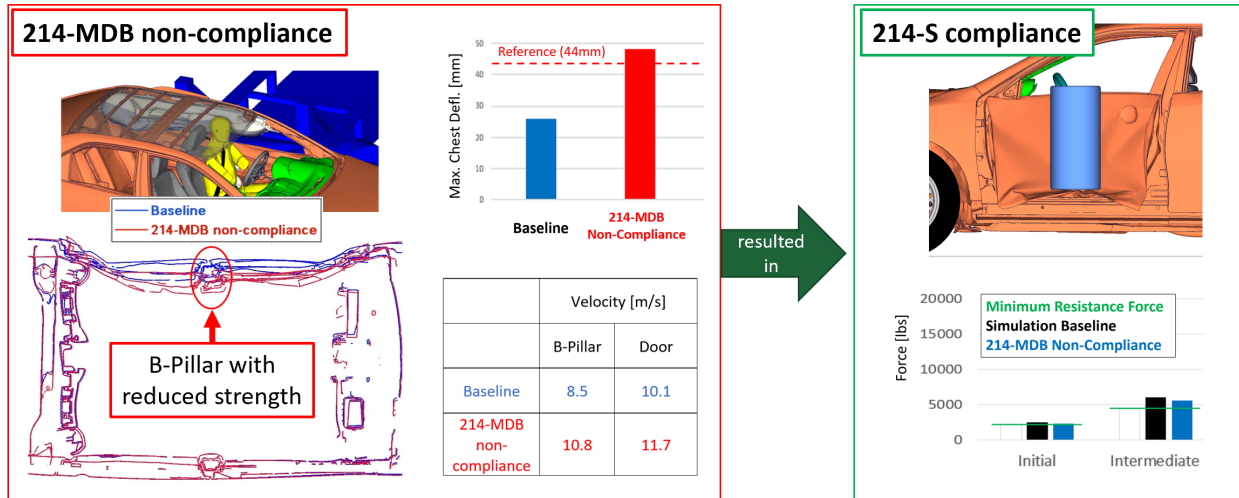


Figure 17. Effect of FMVSS No. 214-MDB non-compliance for 214-S

The model that showed non-compliance for the FMVSS No. 214 MDB configuration was then exercised in the FMVSS No. 214 pole condition, as shown in Figure 18. Structural modifications that resulted in FMVSS No. 214 MDB non-compliance resulted in similar structural deformation in the FMVSS No. 214 pole configuration as the baseline. The maximum exterior crush was marginally higher. Similarly, simulations with a 5th percentile ATD in the driver seat indicated that the maximum combined pelvis force was marginally higher than in the baseline simulation, while clearly below the defined reference criteria.

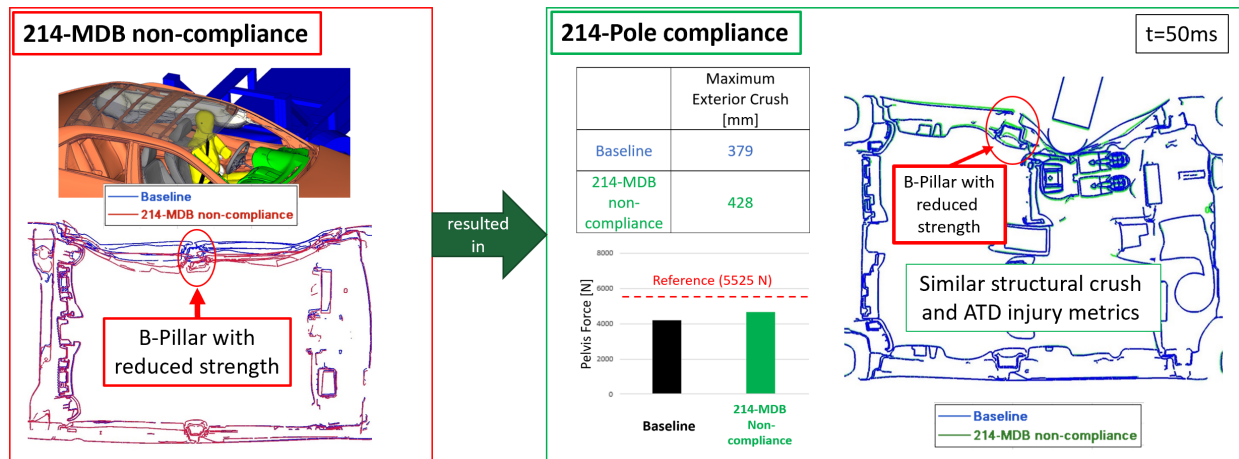


Figure 18. Effect of FMVSS No. 214-MDB non-compliance for 214-Pole

The conducted simulations indicated FMVSS No. 214 pole compliance despite 214-MDB non-compliance. The reduced strength for B-pillar components, that resulted in 214-MDB non-compliance did not significantly affect the performance in the 214-S condition, which mainly relies on the door components. Similarly, it did not significantly affect the performance in the 214-Pole condition, where the vehicle impacts the pole at the front door overlapping with the sill and vehicle floor.

In conclusion, the conducted simulations with a validated sedan FE model indicated FMVSS No. 214-S and pole compliance despite FMVSS No. 214 MDB non-compliance.

3.6 Effect of FMVSS No. 214 Pole Non-Compliance - Sedan

The validated Toyota Camry FE baseline model was then modified in such a way that it showed non-compliance for the FMVSS No. 214 pole configuration. Figure 19 shows the parts with reduced strength in red and yellow, compared to the baseline model. The sill components and the driver seat cross member play an important role for the oblique side pole impact condition. The Toyota Camry and some other vehicles also use an additional reinforcement component, which is specifically designed and positioned for the pole impact configuration, shown in yellow in Figure 19.

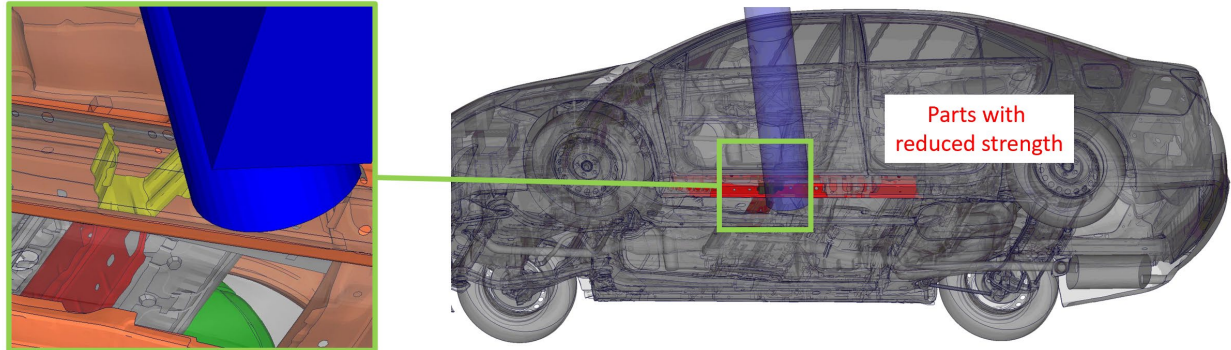


Figure 19. Effect of FMVSS No. 214-S non-compliance for 214-Pole

The applied modifications, documented in Appendix A3, resulted in higher maximum exterior crush and higher occupant pelvis force in the FMVSS No. 214 pole impact, as shown in Figure 20 on the left. The model that showed non-compliance for the FMVSS No. 214 pole configuration was then exercised in the FMVSS No. 214-S static door crush condition, as shown in Figure 20 on the right. Structural modifications that resulted in FMVSS No. 214 pole non-compliance resulted in marginally lower initial and intermediate door crush resistance force levels in the 214-S test configuration. Values were above the minimum required resistance force. The conducted simulations indicated FMVSS No. 214-S static door crush compliance despite dynamic FMVSS No. 214 pole non-compliance.

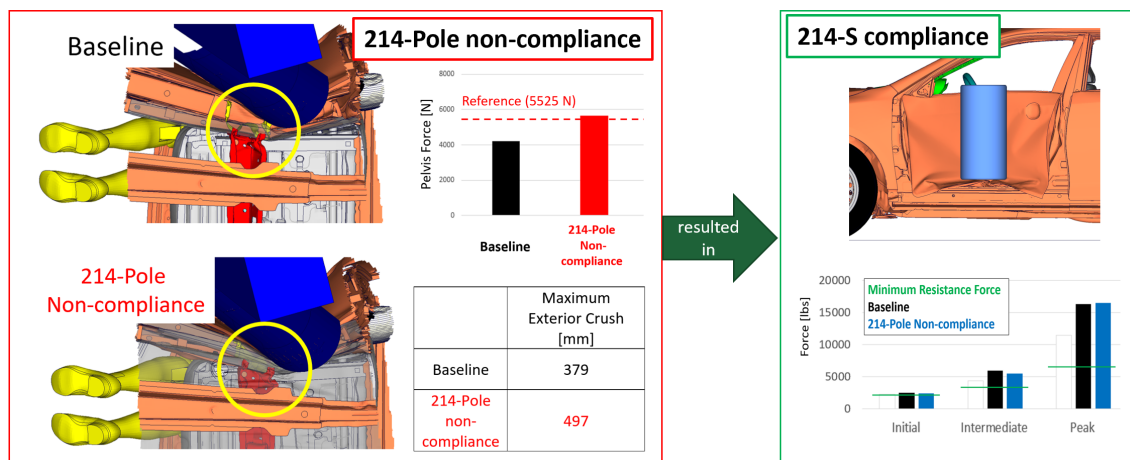


Figure 20. Effect of FMVSS No. 214-Pole non-compliance for 214-S

The model that showed non-compliance for the FMVSS No. 214 pole configuration was then exercised in the FMVSS No. 214 MDB condition, as shown in Figure 21.

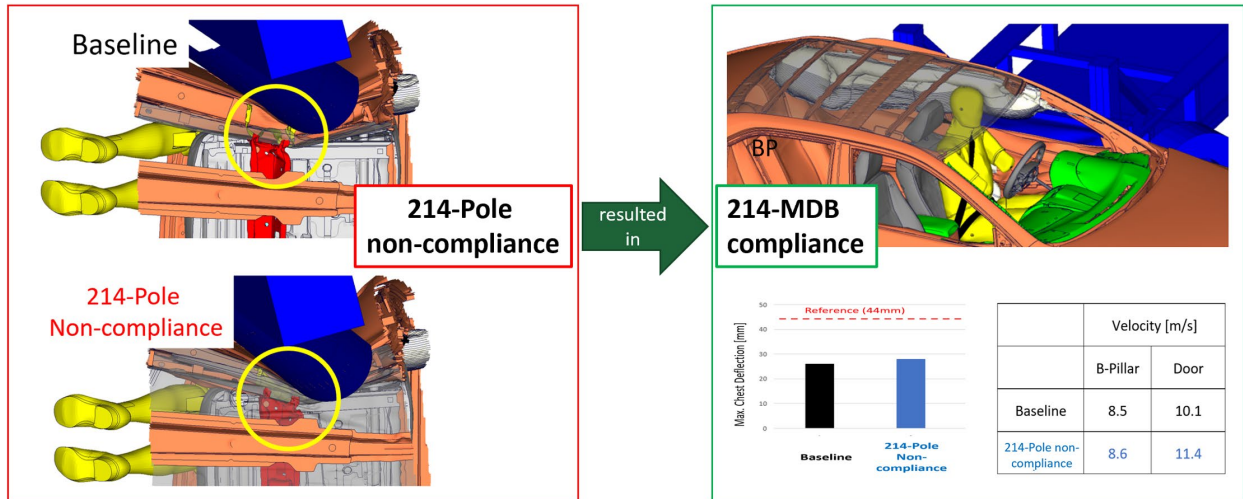


Figure 21. Effect of FMVSS No. 214-Pole non-compliance for 214-MDB

Structural modifications that resulted in FMVSS No. 214 pole non-compliance resulted in similar maximum B-pillar and higher door velocity in the MDB configuration when compared to the baseline simulation. The simulations with a 50th percentile dummy in the driver seat indicated that the maximum chest deflection was marginally higher compared to the baseline simulation, while clearly below the defined reference criteria. The conducted simulations indicated FMVSS No. 214 MDB compliance despite pole non-compliance.

The reduced strength for sill and seat cross member components, that resulted in FMVSS No, 214 pole non-compliance did not significantly affect the performance in the 214-S condition which mainly relies on the door components. Similarly, the 214-MDB condition, which mainly relies on the B-pillar strength, was only affected to an extent that did not result in 214-MDB non-compliance.

In conclusion, the conducted simulations with a validated sedan FE model indicated FMVSS No. 214-S and 214-MDB compliance despite FMVSS No. 214-Pole non-compliance.

3.7 Effect of Vehicle Mass

FMVSS No. 214 MDB requirements apply to multipurpose passenger vehicles, trucks, and buses with a GVWR of less than 6,000 pounds. To understand the effect of different vehicle mass in the dynamic MDB and pole impact configurations, simulations with added weight were conducted. In addition to the baseline simulation with a mass of 3,700 pounds, vehicle masses of 5,000 and 6,000 pounds were analyzed by adding distributed load to the baseline model's structure.

Figure 22 depicts the maximum velocity, measured at the B-pillar in the FMVSS No. 214 MDB configuration. The baseline model with a mass of 3,700; 5,000; and 6,000 pounds is shown in black, dark gray, and light gray, respectively. The modified FE models, that showed FMVSS No. 214 MDB, pole, and 214-S non-compliance are shown in red, blue, and green, respectively. It can be noticed that higher vehicle mass tended to produce marginally lower maximum B-pillar velocity. Higher vehicle mass correlated with higher inertia and therefore tended to produce lower velocities during the FMVSS No. 214 MDB configuration, where the moving barrier

impacts the stationary vehicle. Similar trends were observed for the modified models that showed non-compliance for the MDB, pole, and static conditions.

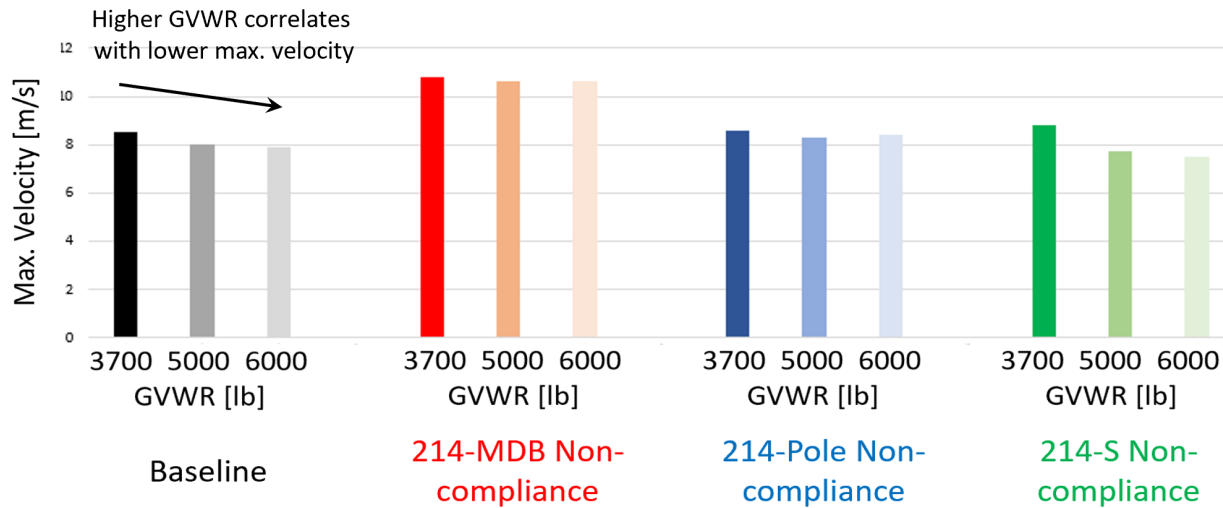


Figure 22. Effect of GVWR for FMVSS No. 214-MDB

Since differences were small, it was concluded that the previously observed tendencies, i.e. FMVSS No. 214-S and 214 pole compliance despite FMVSS No. 214-MDB non-compliance would also hold for different vehicle masses, based on the conducted simulations with the validated sedan vehicle model.

Figure 23 shows the residual maximum exterior crush, measured at the door in the FMVSS No. 214 pole configuration. The baseline model with a mass of 3,700, 5,000, and 6,000 pounds is shown in black, dark gray, and light gray, respectively. The modified FE models, that showed FMVSS No. 214 MDB, pole, and static non-compliance are shown in red, blue, and green colors, respectively. It can be noticed that higher vehicle mass clearly produced larger maximum residual crush, i.e. smaller remaining occupant compartment space for the baseline model. Higher vehicle mass correlated with higher inertia and therefore tended to produce larger deformation during the FMVSS No. 214 pole configuration, where the moving vehicle impacts the stationary rigid pole. Similar trends were observed for the modified models that showed non-compliance for the FMVSS No. 214 MDB, pole, and 214-S conditions.

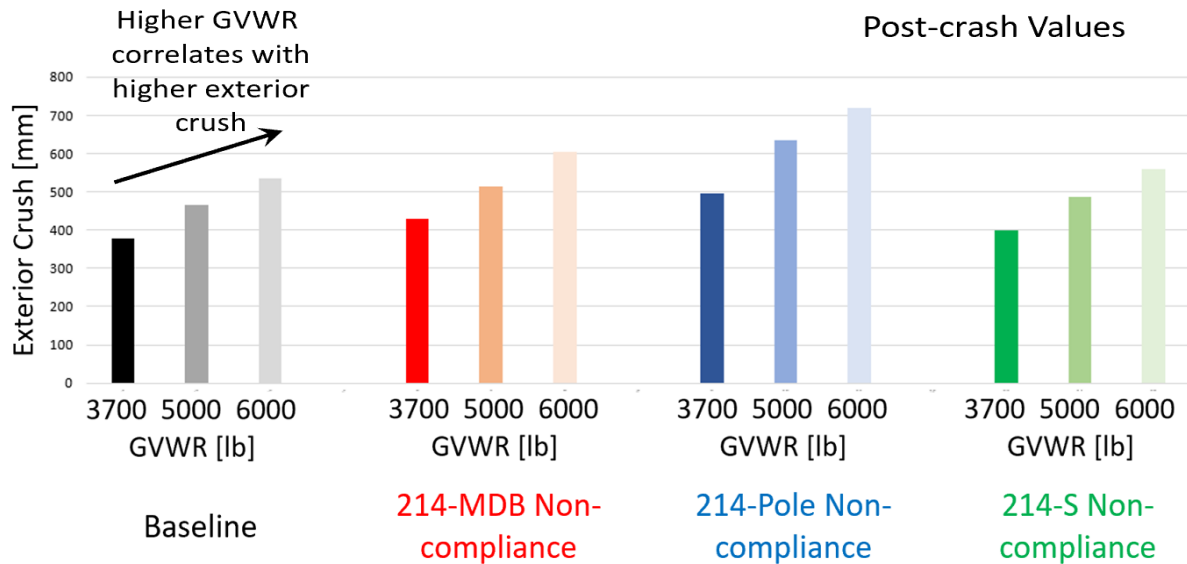


Figure 23. Effect of GVWR for FMVSS No. 214-Pole

Maximum occupant injury metrics typically occur in the early phase of the impact after about 50 milliseconds, as outlined in Chapter 2.3. At this early instant, intrusion levels were comparable for the original and the increased vehicle masses for the baseline and non-compliant vehicle models. Differences ranged between 10 mm and 30 mm compared to about 100 mm for the exterior crush post-crash. The mass effect, especially for the residual exterior crush and related remaining occupant compartment space is clearly more significant for the FMVSS No. 214 pole Non-compliance configuration than for the MDB Non-compliance configuration.

Since FMVSS No. 214 pole compliance is based on ATD metrics, which typically occur early in the crash event, it was concluded that the previously observed tendencies, i.e. FMVSS No. 214-S and dynamic MDB compliance despite FMVSS No. 214 pole non-compliance would hold also for different vehicle masses, based on the conducted simulations with the validated sedan vehicle model.

4. SUV - Nissan Rogue Simulation Study

A 2020 Nissan Rogue was selected as a second vehicle to conduct the FMVSS No. 214 simulation study to understand the effect of mutual non-compliance. It represents the crossover vehicle class, which is a type of SUV with unibody structure.

SUV-type vehicles have significantly different side impact characteristics, especially in the 214-MDB test configuration, due to higher sill and occupant seating position, as shown in Figure 24. SUV vehicles have typically higher seating position than sedans, which affects load-paths and mitigates occupant loads in MDB side impact. It can be noticed from the cross-section view that the MDB honeycomb barrier face geometrically overlaps the entire chest and pelvis region of the occupant seated in the sedan vehicle, as shown in Figure 24 (b), while it only overlaps with the pelvis for the SUV-type vehicle. The bumper typically only partially overlaps with the sedan rocker area and overrides the sill in many cases, making the B-pillar and door the main load paths. In contrast, the MDB bumper directly impacts the SUV's sill area, as highlighted by the red circle in Figure 24 (a), making the rocker and floor structural cross members a more significant load path for the SUV in the 214-MDB side impact configuration, compared to the sedan vehicle class.

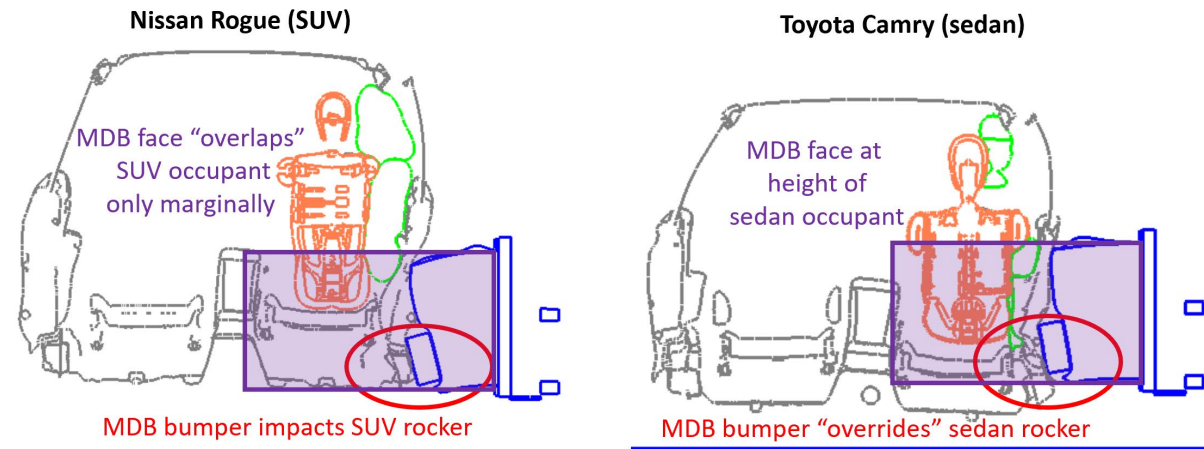


Figure 24. MDB impact location relative to sill and occupant (a) SUV; (b) sedan

Crossover vehicles are often based on platforms shared with passenger cars, in contrast to truck-based SUVs, with bodies on ladder-type frames. The crossover vehicle segment represented by far the largest market share in 2019 with 39.4 percent, as shown in Figure 25 (a). The annual U.S. sales numbers for this vehicle segment increased by 75 percent from 2013 to 2018, as shown in Figure 25 (b).

U.S. light vehicle market in June 2019, by segment

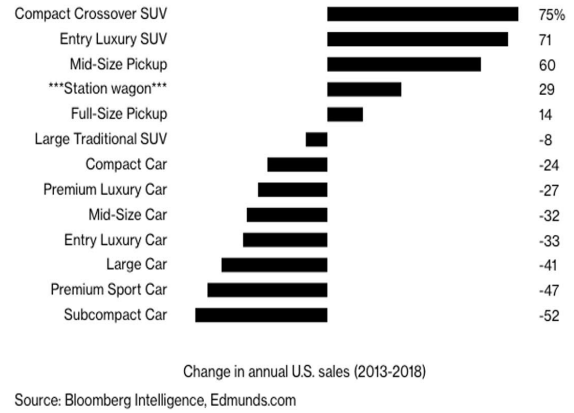
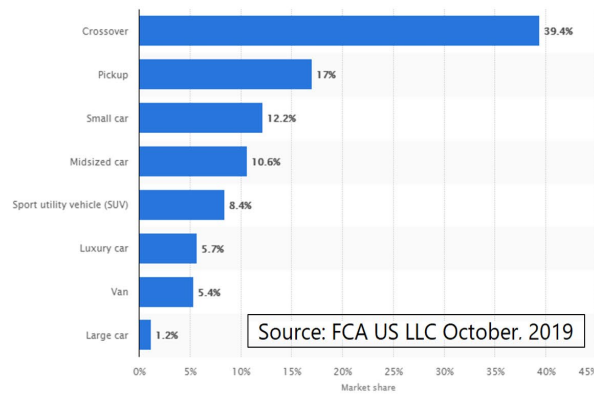


Figure 25. U.S. vehicle segment (a) market share; (b) change in annual sales (2013-2018)

The Nissan Rogue was the vehicle with the second highest U.S. sales numbers in 2018, as shown in Table 1. It has a GVWR of 4,590 pounds, whereas the previously studied 2015 Toyota Camry mid-size sedan has a GVWR of 3,460 pounds.

Table 1. Crossover vehicles with highest U.S. sales number in 2018

Source: FCA US LLC, December 2018

#	Type	Size	Make	Model	Sales	GVWR [lb]
1	CUV	compact crossover SUV	Toyota	RAV4	427,168	4610
2	CUV	compact crossover SUV	Nissan	Rogue	412,110	4590
3	CUV	compact crossover SUV	Honda	CR-V	379,021	4695

The Nissan Rogue received a 5-Star U.S. NCAP side impact rating. Test data for the dynamic FMVSS No. 214 pole and a 62 km/h U.S. NCAP MDB configurations exist. FMVSS No. 214 static door crush tests were conducted in cooperation with TRC. An additional dynamic FMVSS No. 214 MDB test at compliance speed of 54 km/h and an additional dynamic pole impact with a 50th percentile WorldSID, were conducted in cooperation with Calspan.

4.1 SUV - Nissan Rogue FE Model Development

An FE model of a 2020 Nissan Rogue was developed using an established reverse engineering process, as shown in Figure 26. Three physical 2020 Nissan Rogue vehicles were purchased. The first vehicle was used for the FE model development reverse engineering process, such as tear-down and geometry generation. The second vehicle was used to conduct non-destructive suspension tests, vehicle center of gravity (CG) and inertia measurements, and FMVSS No. 214 static door crush tests. Vehicle CG and inertia measurements were determined in cooperation with S-E-A Vehicle Inertia Measurement Facility (VIMF, <https://sealimited.com/capability/center-of-gravity-and-inertia>). The third vehicle was used to conduct the additional dynamic MDB and pole full-scale tests at Calspan.

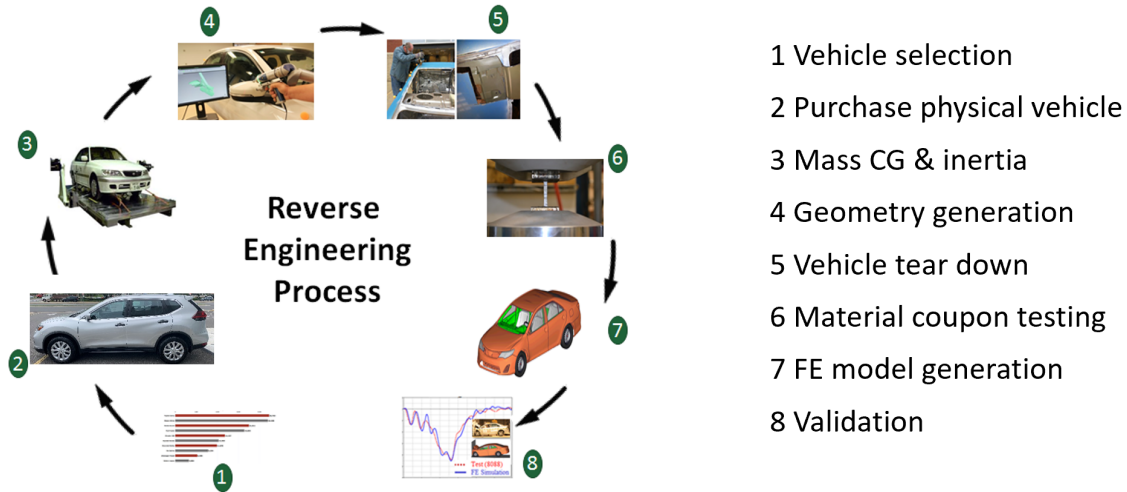


Figure 26. Reverse engineering FE vehicle model development process

Snapshots from the different stages of the vehicle tear down and FE model development process are shown in Figure 27. Thickness of all vehicle parts, as well as type and location of connections were recorded. Material coupons were cut for relevant vehicle components to determine the material characteristics.

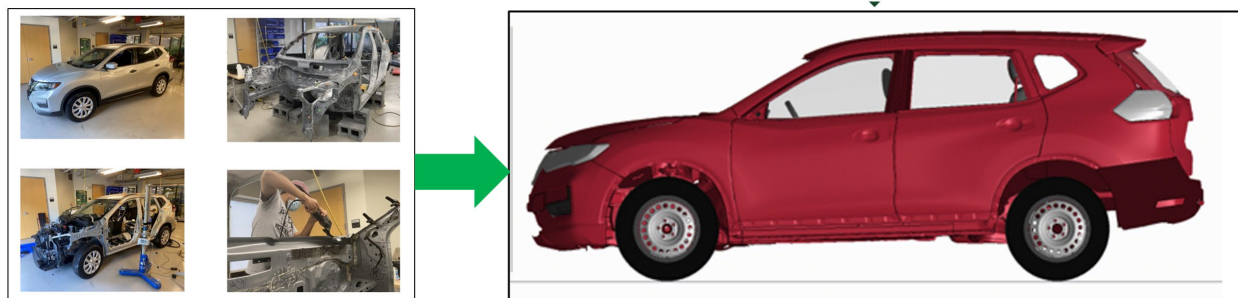


Figure 27. Vehicle tear-down and FE model development process

The validated model, representing the SUV crossover vehicle class with higher sill and occupant seating position, was exercised in a similar manner as the Toyota Camry sedan vehicle, to study the effect of non-compliance for one of the FMVSS No. 214 configurations for the other two FMVSS No. 214 impact conditions.

4.2 SUV - MDB Impact Validation

A FMVSS No. 214 MDB side impact test with a 2020 Nissan Rogue was conducted at Calspan to generate data for FE model validation. The side impact test was conducted in accordance with the Office of Vehicle Safety Compliance’s Laboratory Test Procedure, TP-214D-09 dated September 2012. A 2020 Nissan Rogue SUV was struck on the left side by a MDB, which was moving forward in a 27° crabbed position to the tow road guidance system at a velocity of 52.9 km/h. The target vehicle was stationary and was positioned at an angle of 63° to the line of forward motion. The side impact test was conducted by Calspans Transportation Test Operations Center in Buffalo, New York, on February 22, 2021. Pre-test and post-test photographs of the test vehicle, the MDB, and test dummies were taken.

Test dummies were placed in both the driver and left rear designated seating position according to instructions specified in TP-214D-09. The side impact event was documented by 12 cameras. The WorldSID male dummy was instrumented with triaxial accelerometer packs located in the head with IRTRACC installed in rib and abdomen locations. The SID-II's female dummy was instrumented with triaxial accelerometer packs located in the head and the spine and load cells located in the pubic symphysis and acetabulum.

A perspective view of the conducted FMVSS No. 214 MDB test is shown in Figure 28. The test report and all collected vehicle, barrier, and occupant data has been made available to GMU and NHTSA.



Figure 28. 2020 Nissan Rogue FMVSS No. 214 MDB test

Figure 29 shows the top view of the respective simulation using the developed 2020 Nissan Rogue FE model. Overall vehicle and barrier deformation was well captured, represented by the maximum exterior crush value of 190 mm for the test and 181 mm for the simulation. The y-velocity crash pulse time history data, which is in the dominant impact direction, showed “excellent” correlation represented by a CORA value of 0.96. The velocity time history measured at the CG of the MDB, showed excellent correlation with a CORA value of 0.96, as well.

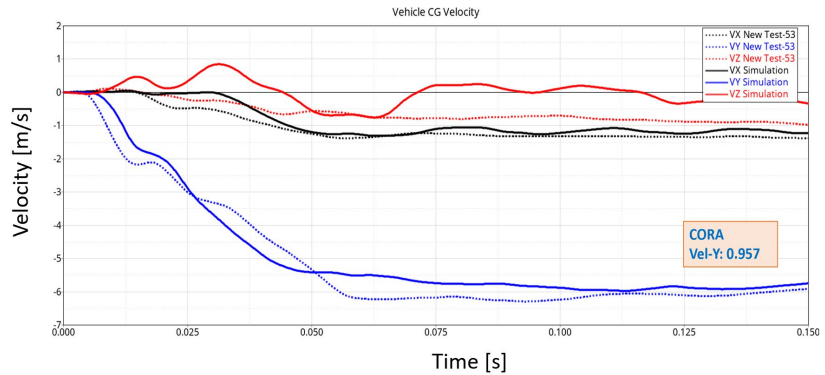
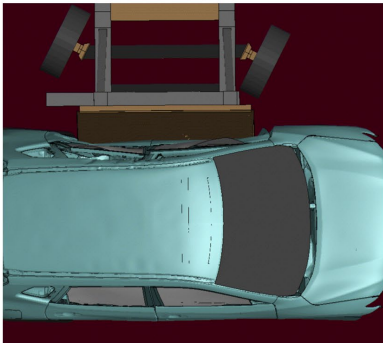


Figure 29. FMVSS No. 214 MDB validation (a) top view; (b) velocity crash pulse

The developed 2020 Nissan Rogue FE model was also exercised at an impact velocity of 62 km/h according to the SINCAP rating procedure and compared to results from an existing full-scale test, NHTSA test #9786. Good correlation of FE model and respective test data was observed for the higher impact speed as well. The maximum exterior crush was 220 mm and 234 mm in test and simulation, respectively. The lateral velocity crash pulse time history compared well, represented by a “good” CORA value of 0.90. The MDB’s velocity pulse time-history showed excellent correlation, characterized by a CORA value of 0.95.

The structural FE model was equipped with relevant interiors and restraints and the state-of-the-art 50-percent WorldSID FE model developed by PDB and distributed by Dynamore and Humanetics. Figure 30 (a) shows a comparison of characteristic values from test and simulation for the 53 km/h configurations. The maximum values compare well for all body regions.

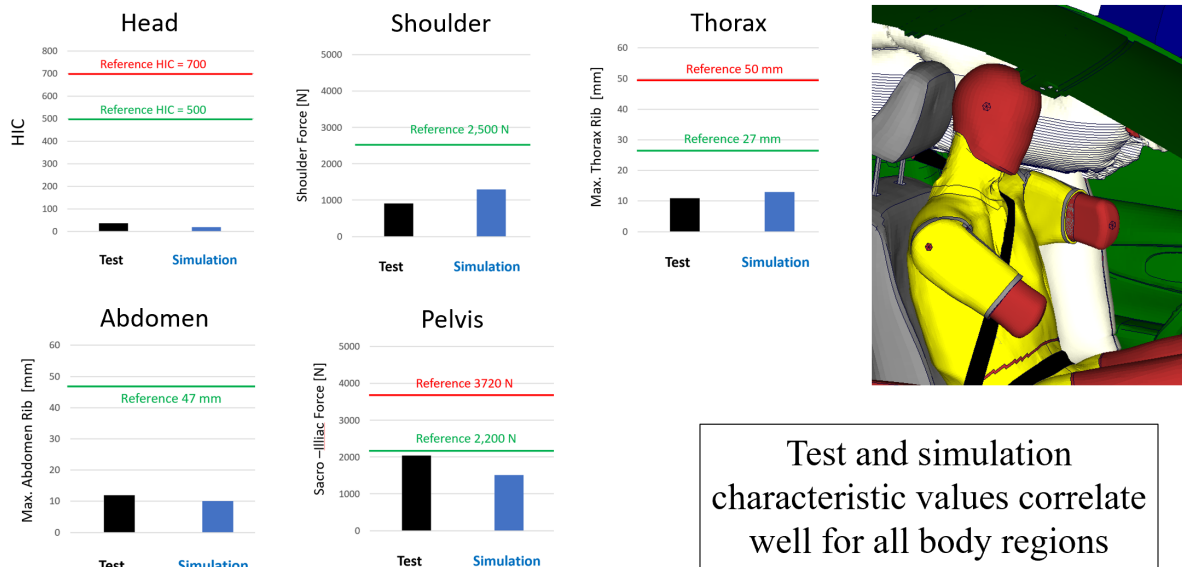


Figure 30.(a) 53 km/h FMVSS No. 214 MDB occupant test versus simulation.

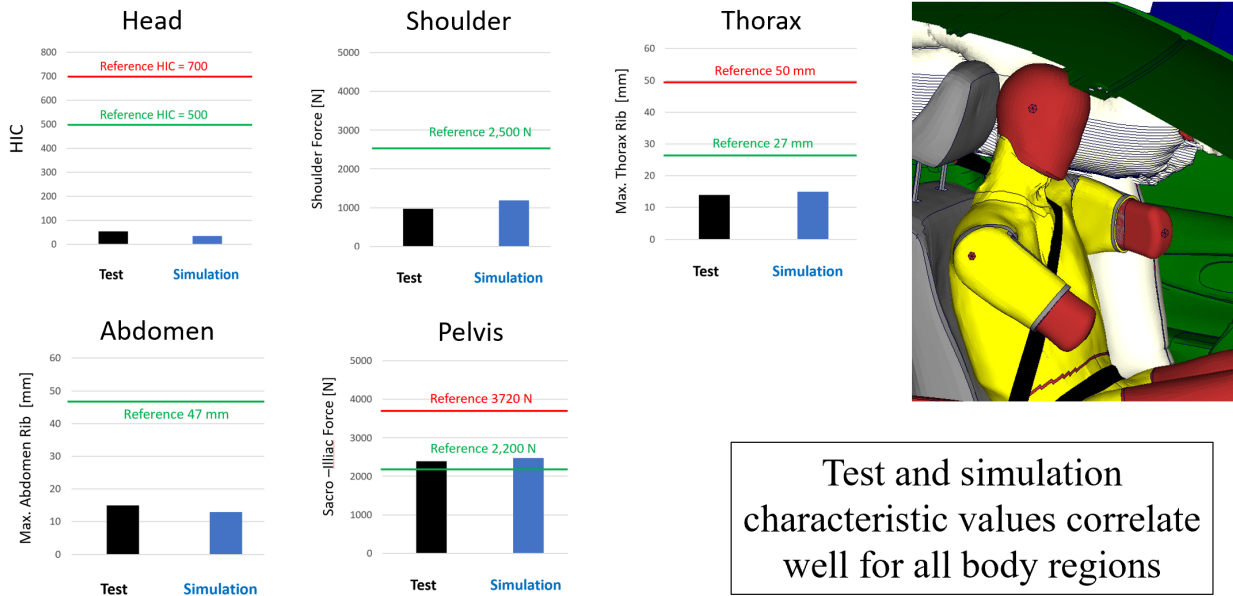


Figure 30. (b) 62 km/h MDB occupant test versus simulation

Figure 30 (b) shows a comparison of characteristic values from test and simulation for the 62 km/h MDB configuration. Again, maximum values compared well for all body regions.

4.3 SUV - Pole Impact Validation

An FMVSS No. 214 pole side impact test with a 2020 Nissan Rogue SUV was conducted at Calspan to generate data for FE model validation. The same vehicle that was previously impacted on the driver side with the MDB at 53 km/h was used. The vehicle showed no structural damage on the passenger side and could therefore be used again to conduct the FMVSS No. 214 pole impact. The side impact test was conducted in accordance with the Office of Vehicle Safety Compliance’s Laboratory Test Procedure, TP-214P-01 dated September 2012. The subject vehicle was towed into the rigid pole at an angle of 75 degrees and a velocity of 31.04 km/h. The test was conducted by Calspan on February 24, 2021. One WorldSID dummy was placed in the front passenger designated seating position according to instructions specified in the TP-214P-01 Test Procedure, dated September 2012. The side impact event was documented by nine High Speed Cameras and one real time camera. The WorldSID male dummy was instrumented with primary and redundant head CG tri-axial accelerometers as well as three-dimensional IR-TRACC (Infrared Telescope Rod for Assessment of Chest Compression), designed to measure abdomen and chest deflections IR-TRACC (Wang & Watson, 2016). All collected vehicle, barrier, and occupant data has been documented, which is available through GMU or NHTSA.

A perspective and side view of the conducted FMVSS No. 214 pole test is shown in Figure 31 (a) and (b), respectively.

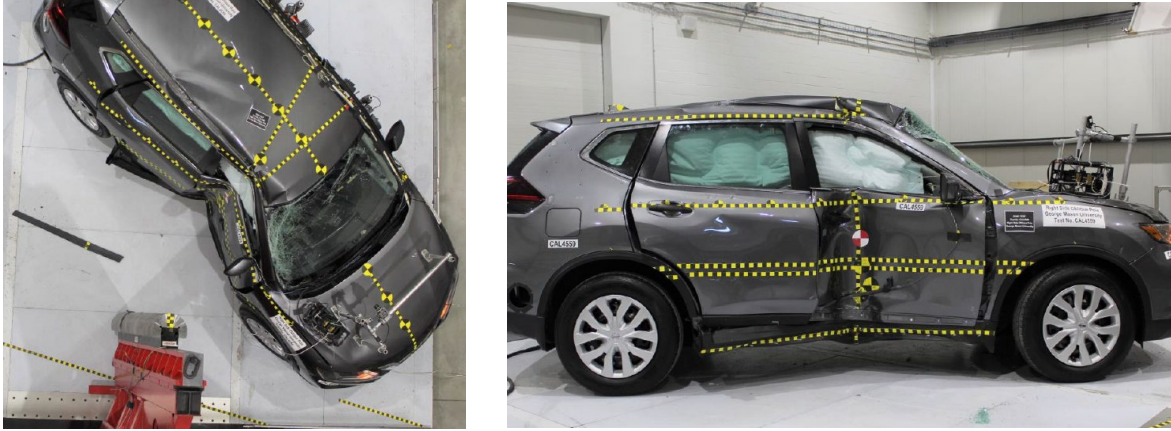


Figure 31. Nissan Rogue FMVSS No. 214 pole post-crash (a) top; (b) side view

Figure 32 (a) shows the velocity crash pulse time history comparisons between test and simulation, which showed “good” correlation for x- and y-pulse based on a CORA value of 0.74 and 0.87, respectively. Figure 32 (b) depicts a top view of the simulation using the developed 2020 Nissan Rogue FE model. Overall vehicle deformation was reasonably well captured, represented by the maximum exterior crush of 420 mm for the simulation and 379 mm for the test. NHTSA test #9780, which was conducted at 32 km/h, showed a maximum exterior crush of 390 mm.

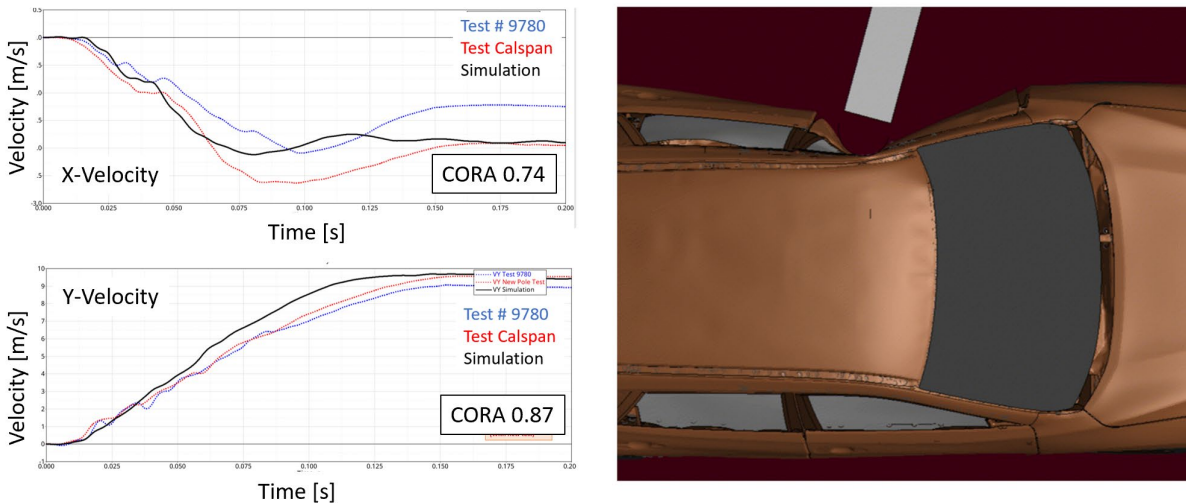


Figure 32. FMVSS No. 214 pole validation (a) velocity crash pulses; (b) top view

4.4 SUV - Static Door Crush Validation

FMVSS No. 214-S requires doors in applicable vehicles to meet minimum force requirements when the doors are quasi-statically loaded with a rigid steel cylinder. Tests at the front and rear door of a 2020 Nissan Rogue were conducted and documented in cooperation with TRC, as shown in Figure 33 (a) and (b).



Figure 33. Nissan Rogue FMVSS No. 214 static post crash (a) front door; (b) rear door

The left front driver door was used to conduct the quasi-static door crush test with seat installed. Figure 34 shows the comparison of test and simulation.

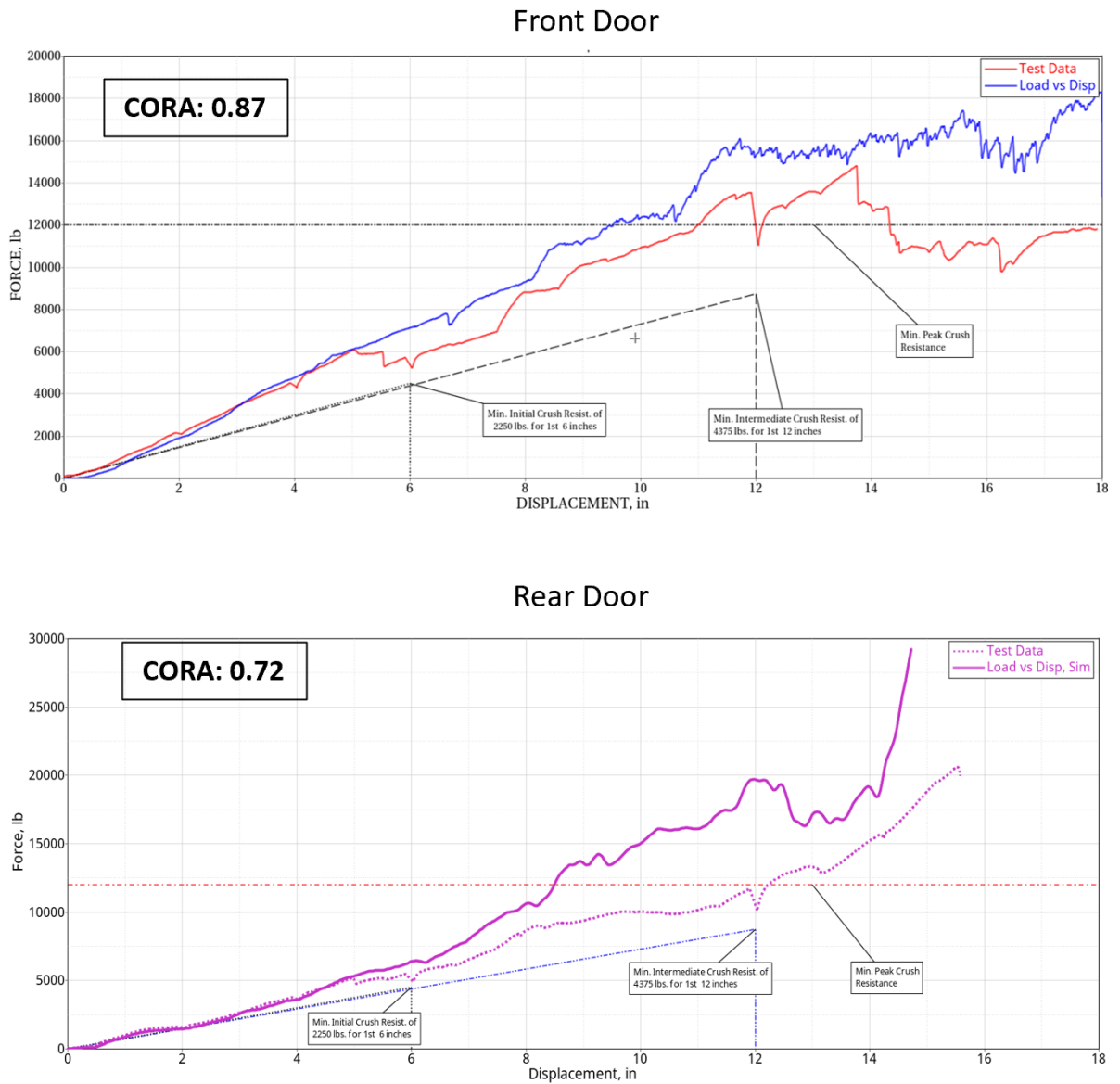


Figure 34. FMVSS No. 214 static door crush validation (a) front; (b) rear door

The entire range of displacement until 18 inches was evaluated. The FE model showed good and acceptable correlation of the force versus displacement time history data, represented by a CORA value of 0.87 and 0.72 for the front and rear door, respectively. Initial, intermediate, and peak resistance forces showed values above the relevant required minimum criteria in test and simulation, as shown in Table 2.

Table 2. Rogue FMVSS No. 214 static door crush resistance forces (a) front; (b) rear door

Front Door				Rear Door			
	Initial Force [lbs]	Intermediate Force [lbs]	Peak Force [lbs]		Initial Force [lbs]	Intermediate Force [lbs]	Peak Force [lbs]
Requirement	2250	4375	12208 *	Requirement	2250	4375	12208 *
Test # 201103	3219	6358	14825	Test # 201102	2725	5744	20624
Simulation	3605	7878	18000	Simulation	2796	7730	29208

* 3.5 times the curb weight of the vehicle (3488 lbs)

The recently developed FE model, representing the crossover SUV vehicle category based on a 2020 Nissan Rogue can be downloaded from GMU/CCSA’s vehicle model website <https://www.ccsa.gmu.edu/models/>.

4.5 2020 Nissan Rogue Suspension Testing

The 2020 Nissan Rogue FE model is anticipated to be used for various research tasks in the future, such as roadside hardware evaluations, for example. Realistic vehicle dynamics and suspension characteristics are important when striking a New Jersey barrier, for instance. To allow the validation of the suspension characteristics, several non-destructive suspension tests have been performed, as shown in Figure 35. Tests were conducted at the FOIL, which is managed by GMU for the Federal Highway Administration.



Figure 35. Nissan Rogue Suspension Testing

Eight tests were conducted at 16 km/h. Speed bumps with different heights of 3.5 and 5 inches were used. Four tests were conducted with the speed bumps located only on the right side of the vehicle and four tests were conducted with the speed bumps located on both, the left and right side. Results from these tests will be used at a later stage to further validate the FE model. This will enhance the models use for roadside hardware evaluations, where suspension characteristics play an important role in capturing the interaction between the vehicle and a guardrail, for example.

4.6 Effect of FMVSS No. 214-S Non-Compliance - SUV

The validated FE baseline model, based on the 2020 Nissan Rogue and representing the SUV vehicle category, was first modified in such a way that it showed non-compliance for the FMVSS No. 214-S static door crush resistance requirement. According to the defined test procedure, the cylindrical impactor does not overlap with the sill of the vehicle. The two door beams, two door outer cross members, and the integrity of the door to B-pillar lock connections were found to have a significant effect on the FMVSS No. 214-S performance. Consequently, non-compliance was achieved by reducing the strength of the door beams and door cross members, as shown in Figure 36 on the left and documented in Appendix B1. The resulting initial resistance force for the first 6 inches of deformation and the intermediate door resistance force between 6 and 12 inches of intrusion using the modified FE model was below the required minimum force criteria, as shown by the red bar in Figure 36 (a). The peak resistance force was also significantly lower than in the baseline simulation, but above the required minimum peak force requirement.

The model that showed non-compliance for the FMVSS No. 214-S test configuration was then exercised in the FMVSS No. 214 MDB condition, as shown in Figure 36 (b). Structural modifications that resulted in FMVSS No. 214-S non-compliance resulted in marginally higher maximum velocity at the B-pillar. Similarly, simulations with a 50th percentile ATD in the driver seat indicated that the maximum chest deflection and pelvis loads were marginally higher, while clearly below defined reference criteria. The conducted simulations indicated FMVSS No. 214 MDB compliance despite 214-S non-compliance for the SUV-type vehicle.

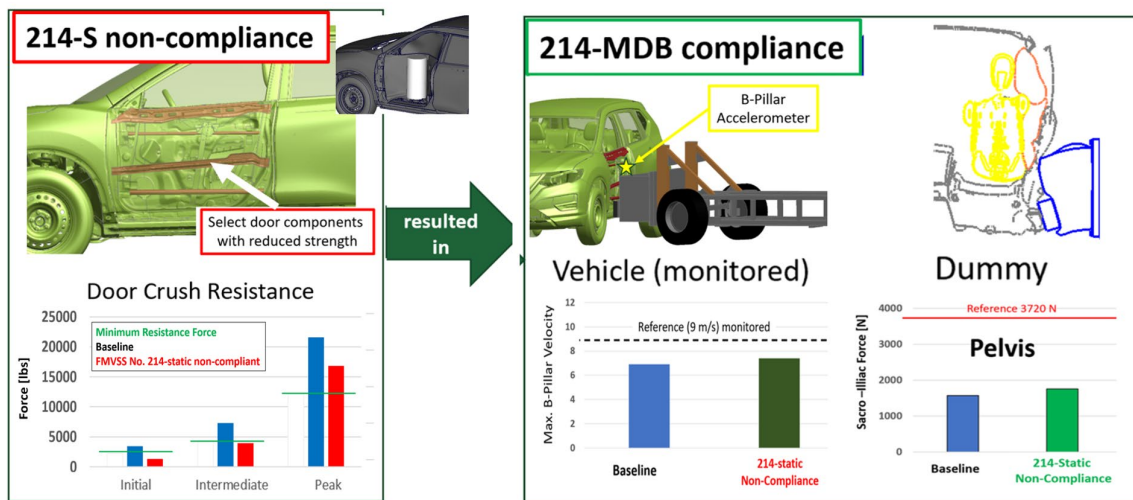


Figure 36. (a) FMVSS No. 214-S non-compliance; (b) effect for 214-MDB load case

The model that showed non-compliance for the FMVSS No. 214-S test configuration was then exercised in the FMVSS No. 214 pole condition, as shown in Figure 37 (b). Structural modifications that resulted in FMVSS No. 214-S non-compliance resulted in similar structural deformation in the 214-pole test configuration. The maximum exterior crush was marginally higher. Similarly, simulations with a 50th percentile ATD in the driver seat indicated that the maximum combined pelvis force was similar to the baseline simulation, clearly below the defined reference criteria. Rocker and floor cross members were found to be the main load path in the pole impact configuration, and roof components also contributed to mitigate deformation.

The structural design changes, which were limited to door components, had therefore only a limited effect for the FMVSS No. 214 pole configuration. The conducted simulations indicated FMVSS No. 214 pole compliance despite 214-S non-compliance.

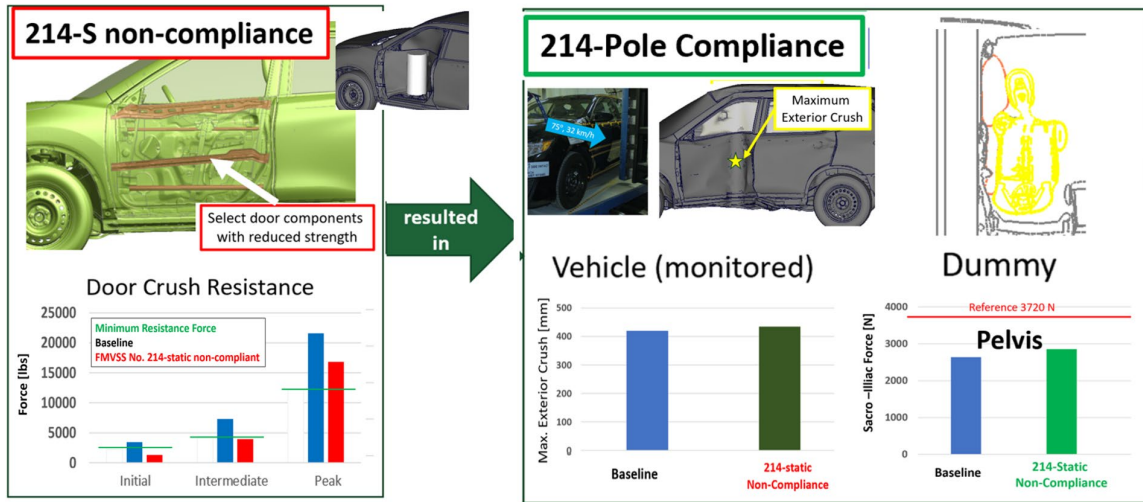


Figure 37. FMVSS No. 214-S non-compliance; (b) effect for pole impact load case

The reduced strength for door components, that resulted in 214-S non-compliance did not significantly affect the performance in the 214-MDB condition, which mainly relies on B-pillar and sill components. Similarly, it did not significantly affect the performance in the 214 pole condition, where the vehicle impacts the pole at the front door overlapping with the sill.

In conclusion, the conducted simulations with a validated SUV FE model indicated FMVSS No. 214 MDB and 214 pole compliance despite FMVSS No. 214-S non-compliance.

4.7 Effect of FMVSS No. 214 MDB Non-Compliance - SUV

The validate Nissan Rogue baseline model was modified in such a way that it showed non-compliance for the FMVSS No. 214 MDB configuration. Figure 38 (a) shows the parts with reduced strength in red. The structural B-pillar components play an important role for the MDB condition like the sedan vehicle class. In addition, due to a significant overlap of the vehicle sill and the barrier bumper, as illustrated in the cross-section view shown Figure 38 (a), the lower door beam and rocker components affected performance in the MDB configuration. Some of the rocker parts extended to the A-pillar. Reducing the material strength and thickness for the components shown in red and documented in Appendix B2, resulted in higher structural deformation and consequently higher occupant loads. The pelvis load for the modified SUV simulation model impacted by the MDB at 53 km/h, represented by the red bar, significantly increased compared to the baseline model, represented by the blue bar. When impacting the modified FE model at the rating speed of 62 km/h, even higher pelvis forces were recorded, as expected, and represented by the dark red bar. The model with significantly increased pelvis forces was considered non-compliant with respect to the FMVSS No. 214 MDB configuration.

The model that showed non-compliance for the FMVSS No. 214 MDB impact was then exercised in the FMVSS No. 214-S static door crush condition, as shown in Figure 38 (b). Structural modifications that resulted in FMVSS No. 214 MDB non-compliance resulted in marginally lower initial and intermediate force levels in the quasi-static configuration. Values

were marginally lower than for the baseline FE model, but clearly above the minimum required resistance force, defined for FMVSS No. 214 compliance. The peak resistance force was clearly above the required force level for the baseline and modified model. The conducted simulations indicated FMVSS No. 214-S door crush resistance force compliance despite dynamic 214-MDB non-compliance.

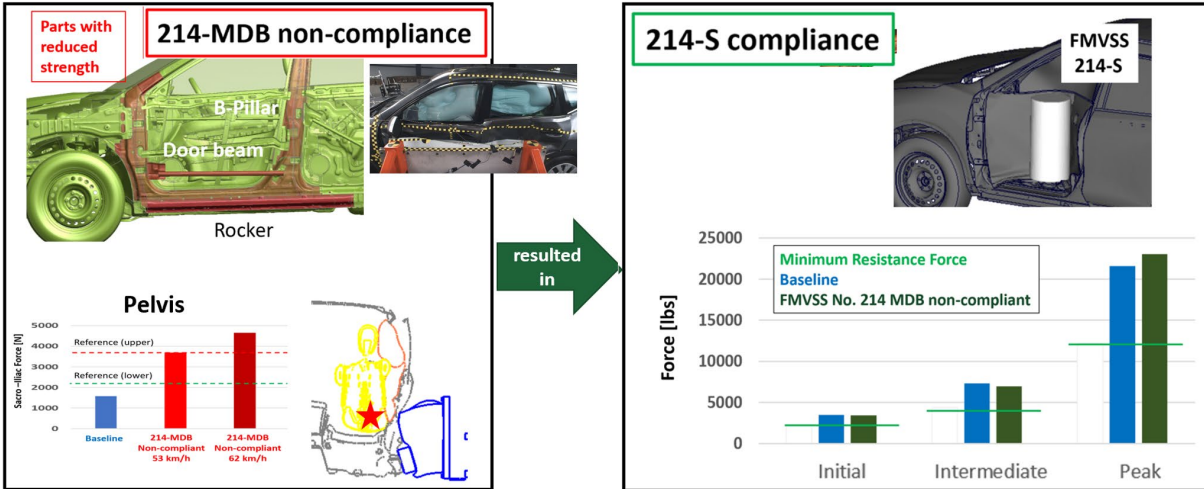


Figure 38. FMVSS No. 214-MDB non-compliance; (b) effect for FMVSS No. 214-S load case

The model that showed non-compliance for the FMVSS No. 214 MDB configuration was then exercised in the FMVSS No. 214 pole condition, as shown in Figure 39 (b). Structural modifications that resulted in FMVSS No. 214-MDB non-compliance resulted in higher structural deformation and pelvis loads in the 214 pole configuration. Simulations with a 50th percentile ATD in the driver seat indicated that the maximum combined pelvis force for the modified model, represented by the brown bar, was significantly higher than in the baseline simulation, represented by the blue bar. It exceeded the reference value, represented by the horizontal, red dashed line.

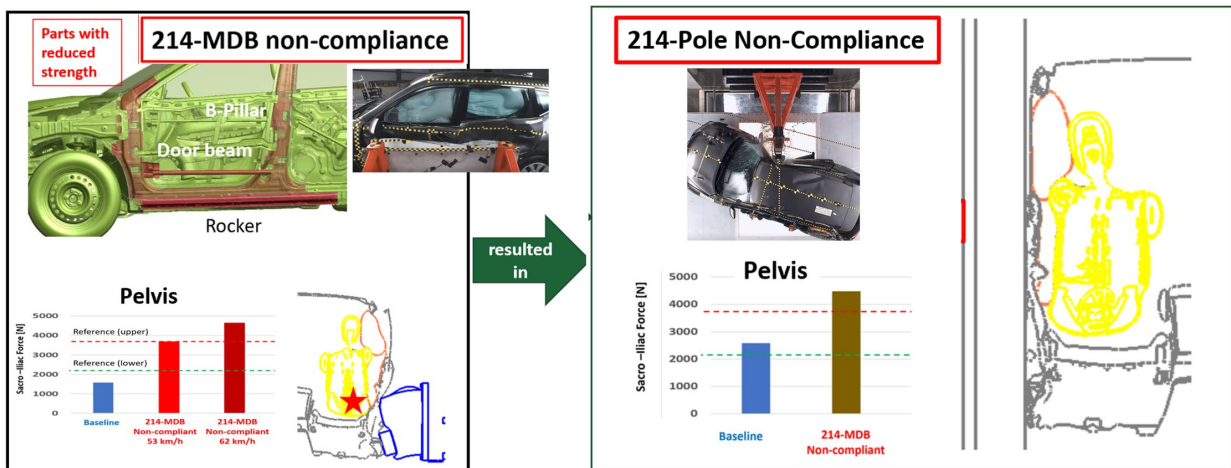


Figure 39. (a) FMVSS No. 214 MDB non-compliance; (b) effect for pole impact load case

The conducted simulations indicated FMVSS No. 214 pole non-compliance for a model that showed 214-MDB non-compliance. The reduced strength for rocker and lower door beam parts in addition to the reduced strength of the B-pillar components, that resulted in 214-MDB non-compliance did not significantly affect the performance in the 214-S condition which mainly relies on the door components. However, it did significantly affect the performance in the 214 pole condition, where the vehicle impacts the pole at the front door overlapping with the sill and vehicle floor. Occupant loads are typically higher in the pole impact configuration than in the MDB configuration for SUV vehicles with higher occupant seating positions, which contributed to the observed effects. While the MDB only marginally overlaps with the occupant, as previously outlined in Figure 24, the rigid pole that extends from the floor to above the roof, can generally cause higher occupant loads for the SUV-type vehicle.

In conclusion, the conducted simulations with a validated SUV FE model indicated FMVSS No. 214-S compliance despite FMVSS No. 214 MDB non-compliance. It also indicated FMVSS No. 214 pole non-compliance for a model that did not comply with FMVSS No. 214 MDB.

4.8 Effect of FMVSS No. 214 Pole Non-Compliance - SUV

The validate 2020 Nissan Rogue SUV FE baseline model was then modified in such a way that it showed non-compliance for the FMVSS No. 214 pole configuration. Figure 40 (a) shows the parts with reduced strength, compared to the baseline model, in red. The sill components and the driver seat cross member play an important role for the oblique side pole impact condition. A combination of weakening these components together with the upper door cross member and lower door bar, select roof parts, and rocker parts that extend to the B-pillar, resulted in non-compliance in the side pole impact configuration. FE model variation details are documented in Appendix B3. This is illustrated by the increased pelvis loads for the modified SUV model, represented by the brown bar in Figure 40 (a), compared to the baseline FE model, represented by the blue bar.

The applied modifications resulted in higher maximum exterior crush and higher occupant pelvis force in the FMVSS No. 214 pole impact, as shown in Figure 40 (a).

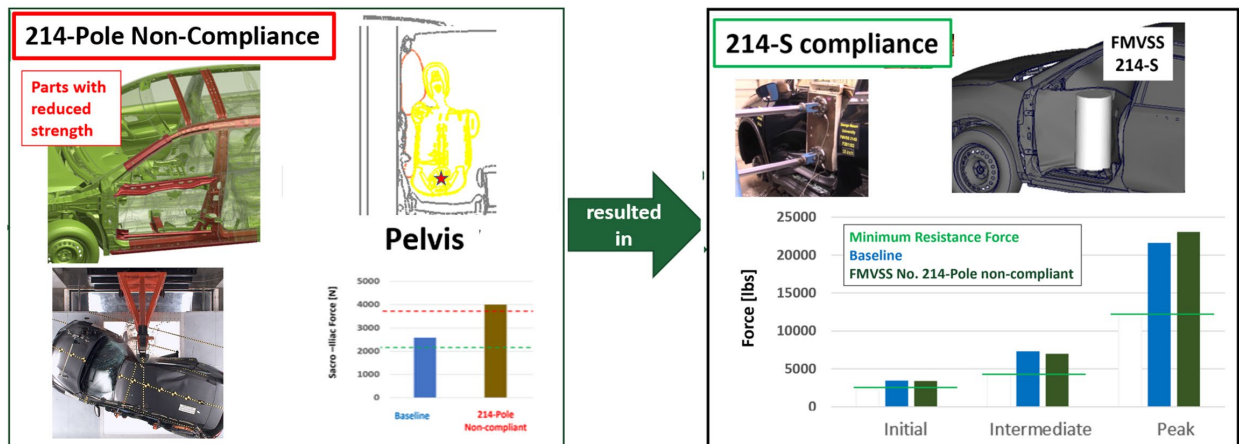


Figure 40. (a) FMVSS No. 214-S non-compliance; (b) effect for 214 Pole load case

The model that showed non-compliance for the FMVSS No. 214 pole configuration was then exercised in the FMVSS No. 214-S static door crush condition, as shown in Figure 40 (b).

Structural modifications that resulted in FMVSS No. 214 pole non-compliance resulted in marginally lower initial and intermediate door crush resistance force levels in the 214-S test configuration. The peak resistance force was clearly above the required force level for the baseline and modified model. All values were above the minimum required resistance force. The conducted simulations indicated FMVSS No. 214-S static door crush compliance despite dynamic FMVSS No. 214 pole non-compliance.

The model that showed non-compliance for the SUV FMVSS No. 214 pole configuration was then exercised in the FMVSS No. 214 MDB condition, as shown in Figure 41 (b).

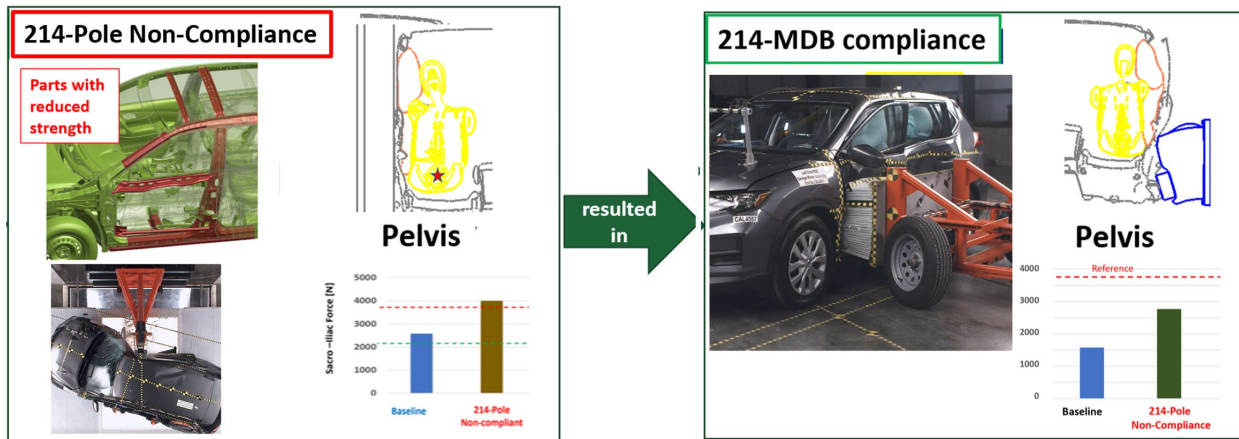


Figure 41. SUV (a) FMVSS No. 214 Pole non-compliance; (b) effect for MDB load case

Structural modifications that resulted in FMVSS No. 214 pole non-compliance resulted in higher structural deformation and velocities also in the MDB configuration when compared to the baseline simulation. B-pillar velocity increased marginally from 8.5 m/s to 8.6 m/s, while the door velocity increased significantly from 10.1 m/s for the baseline model to 11.4 m/s for the model that did not comply with FMVSS No. 214 pole requirements. The simulations with a 50th percentile dummy in the driver seat indicated that the maximum combined sacroiliac pelvis force was significantly higher compared to the baseline simulation. Since the baseline simulation showed a relatively moderate value, which is often the case for SUV-type vehicles in the MDB configuration and even more so for chest load, the pelvic load for the modified model was still clearly below the defined reference criteria. The conducted simulations indicated FMVSS No. 214 MDB compliance despite pole non-compliance.

The reduced strength of relevant sill, roof, door, and B-pillar components, that resulted in FMVSS No. 214 pole non-compliance did not significantly affect the performance in the 214-S condition which mainly relies on the door components. However, it significantly affected the performance in the 214-MDB condition, resulting in higher structural and occupant loads. Due to the relatively low MDB baseline loads, values were below reference criteria resulting in 214-MDB non-compliance for the model that did not comply with FMVSS No. 214 pole.

In conclusion, the conducted simulations with a validated SUV FE model indicated FMVSS No. 214-S and 214-MDB compliance despite FMVSS No. 214 pole non-compliance.

5. Dynamic Performance Measurements as a Surrogate for the Static Test

The objective of this study was to explore options for developing performance criteria so that the FMVSS No. 214 dynamic MDB and/or VTP tests could be used as replacements for the static door crush resistance requirements. Currently, neither of the dynamic 214 test procedures measure door crush resistance force.

5.1 Candidate Dynamic Performance Metrics

Results from the thorough sedan and SUV simulation studies were used to evaluate if it is feasible to use a dynamic performance measurement as a surrogate for the static test. Figure 42 depicts potential structural metrics from the FMVSS No. 214 MDB and pole impact tests.

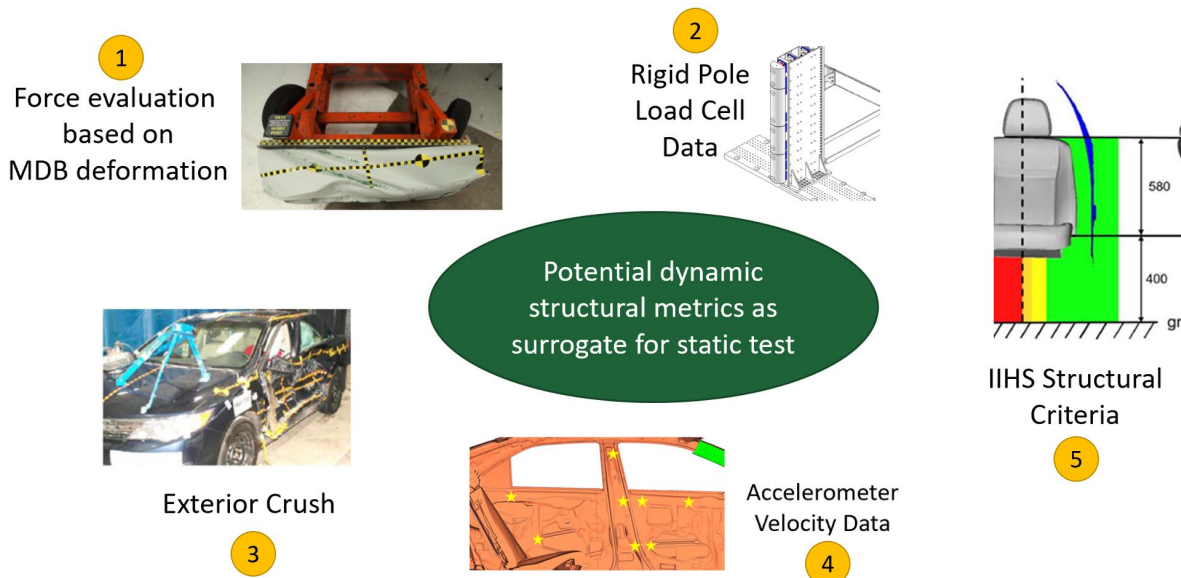


Figure 42. Candidate structural metrics from dynamic tests as surrogate for static test

Deformation, force load cell, and acceleration-based data can be recorded during the dynamic MDB and pole impact configurations:

1. The MDB's honeycomb face has well-defined force-deformation characteristics. Digitizing the MDB barrier surface, pre- and post-crash, allows to calculate the deformation at relevant areas, for example where the door is being struck. From the residual deformation, the force can be calculated. A similar approach has been used for the Progressive Deformable Barrier in frontal offset configurations (Park et al., 2008).
2. Rigid pole load cells at different heights are standard instrumentation during most FMVSS No. 214 pole impact tests. The force time history data combined with vehicle accelerometer data, which can be used to calculate the displacement and deformation of the vehicle exterior, permits generation of a force versus displacement graph, similar to the one used for the FMVSS No. 214-S static door crush resistance tests.
3. Residual exterior crush is typically measured at five different heights of the vehicle, i.e. the sill, the height of the occupant hip point, the mid door location, close to window opening, and at the roof for dynamic FMVSS No. 214 MDB and pole full-scale tests. The

largest exterior crush is observed at the front door in many cases. These residual exterior crush measurements can indicate the structural side impact performance and were considered as candidate metric to indicate door crush resistance.

4. Accelerometer data, specifically absolute velocity time history data recorded at the near-side B-pillar and doors, is a good structural indicator for side impact performance of a vehicle, used by many car manufacturers during the vehicle development process, as outlined in Chapter 2.3.
5. The Insurance Institute for Highway Safety has a well-defined structural criterion that measures the remaining occupant compartment space after a IIHS MDB side impact crash based on B-pillar deformation relative to the middle of the seat.

5.2 Metrics based on Vehicle Accelerometer Data

Velocity time history data derived from accelerometers located at the impact-side B-pillar and doors during a barrier side impact configuration is used by many OEMs as a structural performance metric. In addition to interior design and air bag performance, absolute velocity measured at these locations are an important factor for occupant loads. Occupants positioned in the front and rear seats during a side impact typically do not benefit from the so-called “ride-down.” During frontal impact scenarios, a distinct crash-energy absorption structure, also called frontal crumple zone, causes the vehicle to decelerate more slowly. Occupant loads are then significantly mitigated by the frontal air bags and seat belts before a potentially injurious contact with the vehicle interior occurs. In contrast, the occupants in side impact are more directly loaded by contacting the vehicle’s structure, interiors, and side air bags. Seat and seatbelts can only generate a much smaller ride-down benefit due to the lateral motion.

To determine relevant vehicle metrics for side impact scenarios, it is important to note that vehicle motion relative to the occupant is typically a combination of intrusion and global vehicle kinematics. For example, a vehicle with a low mass can produce high structural velocity in the absence of significant intrusion. From the author’s experience working in industry and with major car manufacturer’s, it is known that quantitative criteria for the structural velocity exist at many OEMs to judge the side impact performance of a vehicle in U.S. NCAP, IIHS, and EuroNCAP side impact barrier configurations.

Accelerometer locations at the middle of the B-pillar and at the door are close to the occupant-to-vehicle contact areas. The B-pillar location can be considered the most reliable accelerometer location with respect to full-scale testing, while the accelerometers at the door, mounted to relatively thin structural components, can produce high oscillations and questionable data. Figure 43 (b) depicts the B-pillar and door accelerometer locations evaluated during the Nissan Rogue simulation study. The results from two simulations were used to evaluate the usability of accelerometer data from the FMVSS No. 214 MDB test as a surrogate for the static test. Maximum absolute velocity values are compared for the SUV baseline model and the model variation that did not comply with the FMVSS No. 214-S static door crush resistance requirement. Note that the maximum velocity at the middle of the B-pillar was identical, as shown in Figure 43 (a), and only marginally higher at the door location, as shown in Figure 43 (c), with values of 6.9 m/s versus 6.7 m/s, for the baseline and 214-static non-compliant model, respectively.

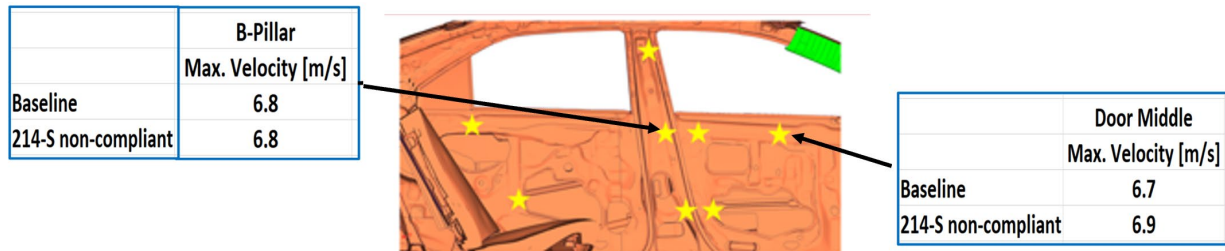


Figure 43. SUV Accelerometer Data - Baseline versus 214-static Non-compliant (a) B-Pillar Velocity; (b) Relevant Locations; (c) Door Velocity

The analyses indicated that accelerometer data from the dynamic MDB configuration is not adequate to serve as a surrogate metric for the static test, due to the different load paths engaged during the FMVSS No. 214 MDB and static door crush tests. This is especially true for the sedan vehicle class, as outlined in the Toyota Camry simulation study presented in Chapter 3. In addition, it was found that SUV-type vehicles with a relatively high rocker location and seating position, has a relatively low barrier to vehicle impact location. This geometric characteristic can produce higher deformations and velocities at the lower part of the vehicle for different structural designs, while deformation and velocities at the middle of the B-pillar and upper door, which are relevant for occupant metrics, are the same or even lower, as shown in Figure 43 (a).

In conclusion, the conducted simulations and respective analyses with validated sedan and SUV FE vehicle models indicated that accelerometer-based velocity time history data from the FMVSS No. 214 dynamic MDB test condition is not adequate to be used as a surrogate for the quasi-static minimum door crush resistance force requirements.

5.3 Metrics based on Vehicle and Barrier Deformation

Vehicle and barrier deformation measurements, including residual MDB honeycomb crush, the IIHS side impact structural criteria, based on B-pillar intrusion and remaining occupant compartment space, and exterior crush measurements available from FMVSS No. 214 MDB and pole tests, as shown in Figure 44, have been evaluated. It was examined if they can indicate door crush resistance forces, as defined in the FMVSS No. 214-S static requirement.

The MDB's honeycomb face has well-defined force-deformation characteristics. Digitizing the MDB barrier surface pre- and post-crash, allows to calculate the deformation at relevant areas, for example where the door is being impacted. From the residual deformation, the resulting force can be calculated.

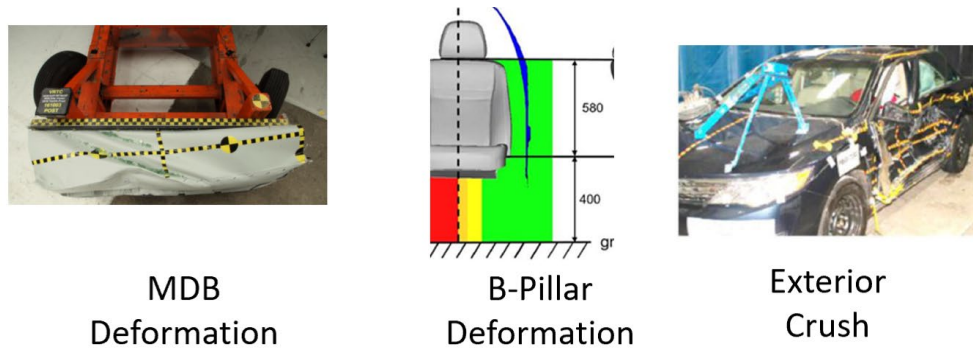


Figure 44. Deformation-based metrics (a) MDB deformation; (b) IIHS structural criteria; (c) exterior vehicle crush

Due to the different load paths engaged for the respective FMVSS No. 214 configurations, no significant difference in honeycomb deformation was observed for the baseline model and the model that did not comply with FMVSS No. 214-S. The MDB configuration for the SUV vehicle category resulted in no significant barrier face deformation for the area impacting the door, since the main load was transferred through the barrier bumper and vehicle rocker area, as shown in Figure 45.



Figure 45. Deformation-based metrics (a) MDB deformation; (b) IIHS structural criteria and exterior vehicle crush

In conclusion, the evaluation of test and simulation results indicated that deformation-based measurements from the FMVSS No. 214 dynamic MDB and pole test conditions have significant limitations to indicate minimum door crush resistance force metrics, as defined in the static test.

5.4 Metrics Based on Rigid Pole Load Cell Data

Locations and contact times between pole and vehicle, as well as between occupant and vehicle, were studied in detail, for the FMVSS No. 214 pole impact test, as shown in Figure 46. After initial contact of the moving vehicle with the stationary rigid pole at 0 ms, the outer door is deformed after about 10 ms and the sill area starts to be impacted and deformed. After 20 ms air

bags are mostly inflated, depending on the sensors used; the door has been significantly crushed, and the sill area is partially deformed at this time. After 40 ms initial contact of the pole with the roof area can occur, depending on the design of a vehicle; air bags have used most of the available package space between occupant and interior to mitigate the impact, and maximum occupant loads start to develop. After 60 ms, the front door and rocker have been significantly deformed at the impact location and the roof area shows deformation to some extent.

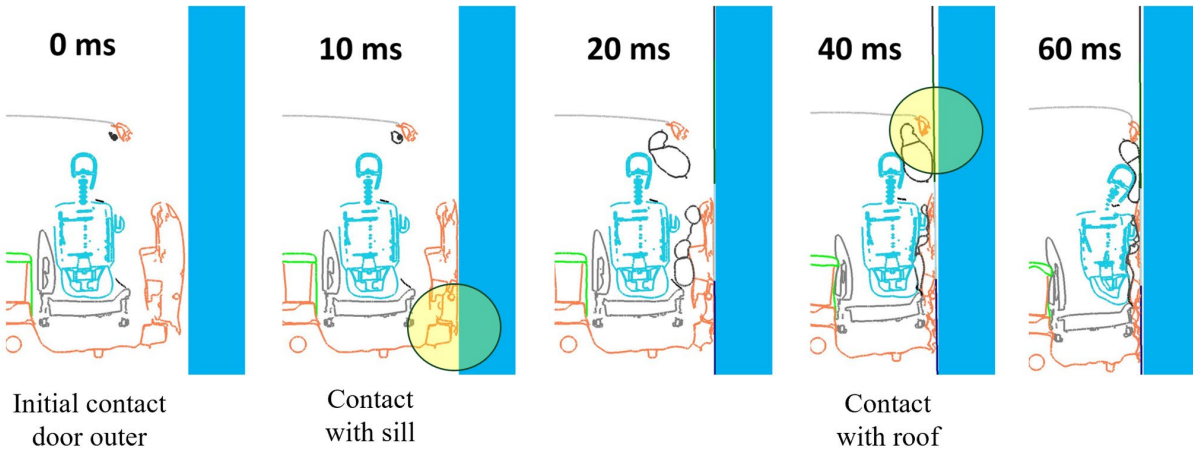


Figure 46. Sequence of FMVSS No. 214 pole characteristic crash events using a crosssection view

These characteristic crash events can clearly be seen in respective load cell data, recorded at different heights of the rigid pole. Figure 47 shows an example of a sedan pole impact with force time-history data recorded at the sill, door, and roof impact areas. The earliest onset can be observed at the door, due to the geometry of the vehicle and the initial contact with the pole in this area. After about 10 ms, a sudden increase in force in the vehicle rocker area can be observed and engagement of the roof area load path can clearly be identified after about 35 ms.

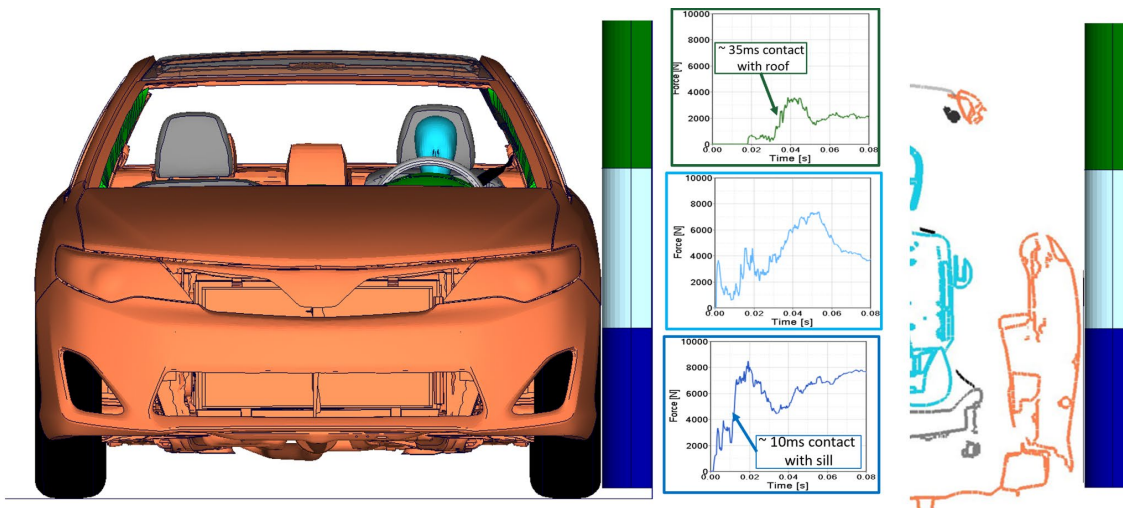


Figure 47. Pole impact force time history data for rocker, door, and roof area

Existing and recorded pole load cell data from full-scale tests and conducted simulations were carefully studied to determine if the dynamic measurements can be used as surrogates for the static test. Figure 48 (a) shows the comparison of the force versus displacement characteristics in

the static door crush resistance condition for Nissan Rogue baseline model and the model that did not comply with FMVSS No. 214-S static requirement. The distinct difference of the resistance force levels for the baseline model, shown in blue, and the model that did not comply with the static requirement, shown in red, can clearly be noticed. Load cell data from the rigid pole instrumentation located next to the front door, as illustrated in Figure 48 (b), was used in combination with vehicle displacement data, to generate a force versus displacement graph, similar to the one used for the static requirement. Figure 48 (c) shows the force versus displacement characteristics for the SUV baseline model and the model that did not comply with the static requirement in the pole impact in blue and red, respectively.

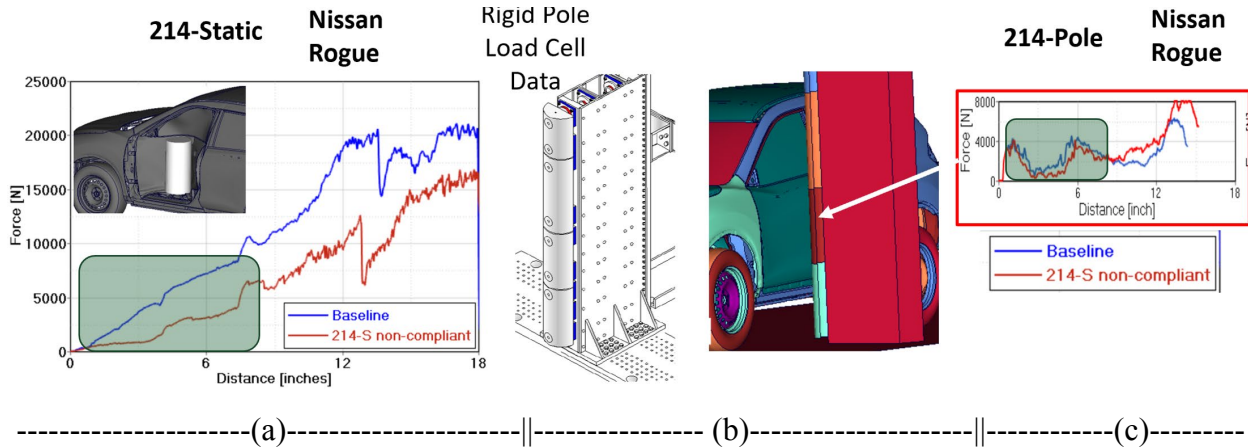


Figure 48. Nissan Rogue baseline versus FMVSS No. 214-S static non-compliant model (a) comparison of static door crush resistance force; (b) load cell locations; (c) comparison of force versus deformation at the door location

From Figure 48 (c), higher maximum exterior crush for the 214-S non-compliant model can be observed. Higher forces can be seen for the baseline model for the first 8 inches of vehicle displacement. This is in qualitative agreement with the force versus displacement characteristics observed in the static door crush condition. Vehicle deformation at the sill and roof affect the loads induced into the door in the pole configuration, in contrast to the static door crush test, where the rigid cylinder intrudes into the door exclusively. Therefore, force versus displacement characteristics for static cylinder and dynamic pole tests, did not show the same qualitative trend after about 8 inches of crush for the baseline model and the FMVSS No. 214-S non-compliant model.

In conclusion, the evaluation of rigid pole load cell data measurements showed that they can qualitatively indicate front door crush resistance to some extent, similar to the FMVSS No. 214-S test condition, in the initial deformation phase, but has limitations for higher intrusions.

5.5 Surrogate Metrics Limitations

As outlined in the previous chapters, there are significant limitations of using performance measurements from the dynamic FMVSS No. 214 MDB and pole configurations as a surrogate for the static door crush requirement:

- The most obvious limitation is the lower maximum exterior crush, which was about 8.7 inches and 13.7 inches for recent MDB and pole impact full-scale tests, respectively. In contrast, the static door crush test requires front and rear door crush resistance force to be evaluated up to 18 inches of deformation.
- Accelerometer based velocity time history data, which can be a good indicator for side impact performance of a vehicle with respect to occupant metrics, has significant limitations. Different load paths, relevant for the static and dynamic tests, especially for sedan-type vehicles, and characteristic deformation patterns with higher seating positions for SUV-type vehicles, make this dynamic measure not adequate to be used as a surrogate for the quasistatic test.
- Smaller maximum exterior crush was observed for the dynamic FMVSS No. 214 MDB and pole conditions compared to the static requirement. Limited engagement and deformation of upper honeycomb face, especially for “higher” SUV-type vehicles where the MDB bumper engages with the rocker also presented significant limitations. The exterior crush, MDB deformation, and IIHS structural criteria were therefore found not adequate to serve as surrogate measurements for the static test.
- The evaluation of rigid pole load cell data measurements showed that they can qualitatively indicate front door crush resistance to some extent, similar to the FMVSS No. 214-S test condition, in the initial deformation phase, but has limitations for higher intrusions.

Additional limitations, to the ones outlined for the front door, exist for defining a performance metric based on results from the dynamic FMVSS No. 214 MDB and pole configurations, that can be used as surrogate for the static door crush test at the rear door. Pole impacts are only performed at the front door and, therefore, do not provide any data that could indicate the door crush resistance of the rear doors. Similarly, the MDB is positioned relative to the front axis of a vehicle and typically impacts the B-pillar, the entire front door, but only part of the rear door, depending on the wheelbase and length of a vehicle.

6. Conclusion

A validated FE model representing the sedan vehicle category and a validated FE model representing the SUV vehicle type were used to conduct simulation studies that investigated the mutual effect of non-compliance for each of the three FMVSS No. 214 side impact configurations, the quasi-static door crush test, the MDB barrier impact, and the pole configuration.

A validated FE model of a 2015 Toyota Camry was used to conduct the sedan FMVSS No. 214 Simulation Study. The baseline FE model was modified in such a way, that it resulted in non-compliance with respect to the FMVSS No. 214-S test configuration, based on minimum door crush resistance force requirements. Similarly, FE models were generated, that resulted in non-compliance for the dynamic FMVSS No. 214-MDB and 214 pole impact configurations, based on ATD metrics.

It was found that the three FMVSS No. 214 configurations mainly rely on different vehicle structural areas, as shown in Figure 49.

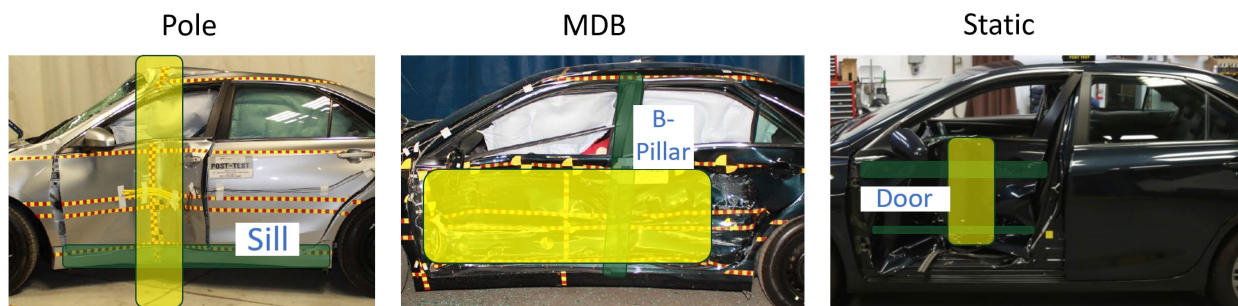


Figure 49. Main load paths during FMVSS No 214 (a) pole; (b) MDB; and (c) static door crush

(1) FMVSS No. 214-S static door crush, where a cylindric impactor does not overlap with the sill or the B-pillar, is mainly affected by door strength characteristics; (2) FMVSS No. 214-MDB, where the moving barrier only marginally overlaps with the sill of a sedan vehicle, is mainly affected by B-pillar strength and deformation characteristics; and (3) FMVSS No. 214 pole, where the moving vehicle impacts the stationary rigid pole at the front door, is mainly affected by sill and adjacent reinforcement components. Consequently, it was found that structural modifications that resulted in non-compliance for one of the FMVSS No. 214 impact configurations did not result in non-compliance for the other two configurations.

A FE model of a 2020 Nissan Rogue SUV was developed applying an established reverse engineering process and used to conduct a similar simulation study, as for the Toyota Camry sedan. It was found that structural modifications that resulted in non-compliance for one of the load cases did not result in non-compliance for the other two configurations, except for 214-MDB non-compliance, which also resulted in 214 pole non-compliance.

Different metrics from the FMVSS No. 214 MDB and pole side impact configurations were evaluated to determine the feasibility of using dynamic performance measurements as a surrogate for the FMVSS No. 214 static door crush test. It was found that there are significant limitations, because of the different main load paths relevant for the dynamic and static side impact tests. Dynamic rigid pole load cell data showed the highest potential of indicating initial door crush resistance.

7. References

- Barbat, S., Fu, Y., Zhan, Z., Yang, R.-J., & Gehre, C. (2013, May 27-30). *Objective rating metric for dynamic systems* (Paper Number 13-0448). 23rd Enhanced Safety of Vehicles Conference, Seoul, Republic of Korea.
- Park, C.-K., Hong, S.-W., Mohan, P., Morgan, R. M., Kan, C.-D., Lee, K., Park, S., & Bae, H. (2016). *Simulation of progressive deformable barrier (PDB) tests*. 10th International LS-DYNA Users Conference, Detroit, MI, June 8-10, 2008.
- Reichert, R., Mohan, P., Marzougui, D., Kan, C., & Brown, D. (2016, April 12-14), *Validation of a Toyota Camry finite element model for multiple impact configurations* (SAE Technical Paper 2016-01-1534). SAE 2016 World Congress and Exhibition, Detroit, MI. doi:10.4271/2016-01-1534.
- Reichert, R., & Kan, C.-D. (2017, May 9-11), *Development of a 2015 mid-size sedan vehicle model*. 11th European LS-DYNA conference, Salzburg, Austria.
- Reichert, R. (2021, February 2-3). *Crash simulation of FMVSS No. 214 safety performance*. [PowerPoint presentation]. 2021 SAE Government/Industry Digital Summit, USA [Digital, no location]. <https://www.nhtsa.gov/node/103701>
- Thunert, C. (2012), *CORA Release 3.6 User's Manual*, Version 3.6. GNS mbH, and Partnership for Dummy Technology and Biomechanics.
- Wang, Z., & Watson, B. (2016). *An algorithm to calculate chest deflection from 3D IR-TRACC* (SAE Technical Paper 2016-01-1522). SAE International. doi:10.4271/2016-01-1522

Appendix A. Toyota Camry FE Model Variations



M1: Camry Baseline			M2: Camry Static Non-Compliant		
Part Image	Part ID	Thickness [mm]	Part Image	Part ID	Thickness [mm]
	2000868	2.7		2000868	0.95

Figure A-1. Toyota Camry FMVSS No. 214 static non-compliant versus baseline model















M1: Camry Baseline			M2: Camry MDB Non-Compliant		
Part Image	Part ID	Thickness [mm]	Part Image	Part ID	Thickness [mm]
	2000230	1.6		2000230	0.5
	2000288	1.5		2000288	0.5
	2000292	1.65		2000292	0.5
	2000293	2		2000293	0.5
	2000298	1.6		2000298	0.5
	2000312	1.85		2000312	0.5
	2001057	1.5		2001057	0.5

Figure A-2. Toyota Camry FMVSS No. 214 MDB non-compliant versus baseline model











M1: Camry Baseline			M2: Camry Pole Non-Compliant		
Part Image	Part ID	Thickness [mm]	Part Image	Part ID	Thickness [mm]
	2000221	0.9		2000221	0.5
	2000222	1.4		2000222	0.5
	2000224	1.45		2000224	0.5
	2000293	2		2000293	0.5
	2000303	3		2000303	0.5

Figure A-3. Toyota Camry FMVSS No. 214 pole non-compliant versus baseline model

Appendix B. Nissan Rogue FE Model Variations

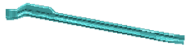
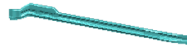






M1: Rogue Baseline			M2: Rogue Static Non-Compliant		
Part Image	Part ID	Thickness [mm]	Part Image	Part ID	Thickness [mm]
	2000105	0.58		2000105	0.3
	2000106	2.0		2000106	0.3
	2000111	2.2		2000111	0.3
	2000101	0.7		2000101	0.3

Figure B-1. Nissan Rogue FMVSS No. 214 static non-compliant versus baseline model



















M1: Rogue Baseline				M2: Rogue MDB Non-Compliant			
Part Image	Part ID	Yield Strength [N/mm]	Thickness [mm]	Part Image	Part ID	Yield Strength [N/mm]	Thickness [mm]
	2000106	800	2		2000106	800	0.5
	2000178	500	1.31		2000178	250	0.5
	2000294	400	1.37		2000294	250	0.5
	2000052	675	1.205		2000052	250	0.5
	2000139	500	1.07		2000139	250	0.5
	2000053	500	1.4		2000053	250	0.5
	2000286	400	1.406		2000286	250	0.5
	2000033	360	0.938		2000033	360	0.4
	2000326	400	1.33		2000326	250	0.5

Figure B-2. Nissan Rogue FMVSS No. 214 MDB non-compliant versus baseline model







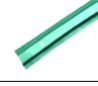
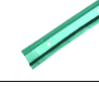
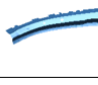
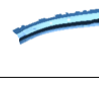




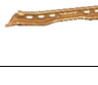
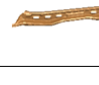












M1: Rogue Baseline				M2: Rogue Pole Non-Compliant			
Part Image	Part ID	Yield Strength [N/mm]	Thickness [mm]	Part Image	Part ID	Yield Strength [N/mm]	Thickness [mm]
	2000022	360	0.73		2000022	250	0.5
	2000023	360	1.19		2000023	250	0.5
	2000033	360	0.938		2000033	250	0.7
	2000034	360	1.36		2000034	250	1
	2000035	450	1.01		2000035	250	0.6
	2000036	360	1.44		2000036	250	0.9
	2000052	675	1.205		2000052	250	0.5
	2000101	360	0.7		2000101	250	0.4
	2000106	800	2.19		2000106	250	1
	2000122	250	1.35		2000122	250	1.35
	2000139	500	1.07		2000139	250	0.6
	2000286	500	1.406		2000286	250	0.5
	2000294	400	1.37		2000294	250	0.5
	2000872	360	1.1		2000872	250	0.6

Figure B-3. Nissan Rogue FMVSS No. 214 pole non-compliant versus baseline model

DOT HS 813 276
September 2022



U.S. Department
of Transportation
**National Highway
Traffic Safety
Administration**

